REVIEW

www.the-innovation.org

All-temperature area battery application mechanism, performance, and strategies

Siqi Chen,[1,2] Xuezhe Wei,[1] Guangxu Zhang,[1] Xueyuan Wang,[1] Jiangong Zhu,[1] Xuning Feng,[2,*] Haifeng Dai,[1,*] and Minggao Ouyang[2]
*Correspondence: fxn17@mail.tsinghua.edu.cn (X.F.); tongjidai@tongji.edu.cn (H.D.)
Received: February 27, 2023; Accepted: June 19, 2023; Published Online: June 21, 2023; https://doi.org/10.1016/j.xinn.2023.100465

GRAPHICAL ABSTRACT

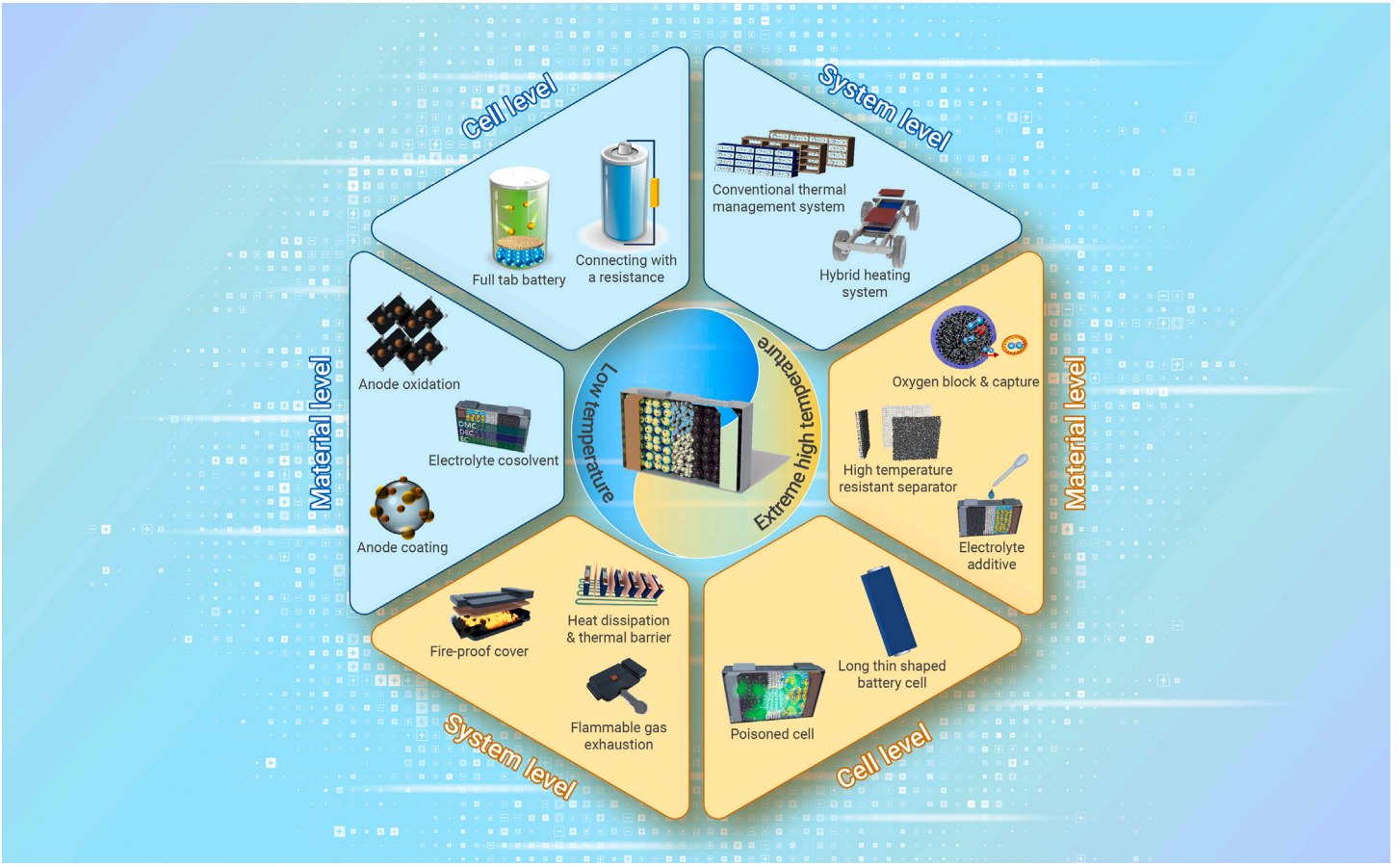

PUBLIC SUMMARY

- Mechanism-temperature map reveals all-temperature area battery reaction evolution.
- Battery performance and safety issues are clarified from material, cell, and system levels.
- Strategy-temperature map proposes multilevel solutions for battery applications.
- Future perspectives guide next generation high performance and safety battery design.

REVIEW

All-temperature area battery application mechanism, performance, and strategies

Siqi Chen,[1,2] Xuezhe Wei,[1] Guangxu Zhang,[1] Xueyuan Wang,[1] Jiangong Zhu,[1] Xuning Feng,[2,*] Haifeng Dai,[1,*] and Minggao Ouyang[2]

[1]Clean Energy Automotive Engineering Center, Tongji University, Shanghai 201804, China

[2]State Key Laboratory of Automotive Safety and Energy, Tsinghua University, Beijing 100084, China

*Correspondence: fxn17@mail.tsinghua.edu.cn (X.F.); tongjidai@tongji.edu.cn (H.D.)

Received: February 27, 2023; Accepted: June 19, 2023; Published Online: June 21, 2023; https://doi.org/10.1016/j.xinn.2023.100465

Citation: Chen S., Wei X., Zhang G., et al., (2023). All-temperature area battery application mechanism, performance, and strategies. The Innovation **4(4)**, 100465.

Further applications of electric vehicles (EVs) and energy storage stations are limited because of the thermal sensitivity, volatility, and poor durability of lithium-ion batteries (LIBs), especially given the urgent requirements for all-climate utilization and fast charging. This study comprehensively reviews the thermal characteristics and management of LIBs in an all-temperature area based on the performance, mechanism, and thermal management strategy levels. At the performance level, the external features of the batteries were analyzed and compared in cold and hot environments. At the mechanism level, the heat generation principles and thermal features of LIBs under different temperature conditions were summarized from the perspectives of thermal and electrothermal mechanisms. At the strategy level, to maintain the temperature/thermal consistency and prevent poor subzero temperature performance and local/global overheating, conventional and novel battery thermal management systems (BTMSs) are discussed from the perspective of temperature control, thermal consistency, and power cost. Moreover, future countermeasures to enhance the performance of all-climate areas at the material, cell, and system levels are discussed. This study provides insights and methodologies to guarantee the performance and safety of LIBs used in EVs and energy storage stations.

INTRODUCTION

The carbon neutrality proposal has promoted clean energy development in recent years.[1,2] Electric vehicles (EVs) are investigated as the appropriate replacement for the conventional internal combustion engine-based vehicle to reduce greenhouse gas emissions and pollution, such as carbon dioxide (CO_2).[3] As a renewable power source, batteries make the EV efficient and environmentally friendly.[4,5] Different types of battery technologies have been proposed, such as lithium-ion batteries (LIBs), lead acid batteries, nickel-based batteries, and sodium-based batteries.[6] However, with the worldwide electrification trend, LIB has become predominant in electronics, EVs, and energy storage stations, with superior properties of higher energy density and long lifespan.[7–9] These industries call for better batteries with lower cost, fast charging rates, and enhanced subzero temperature performance/thermal stability in next-generation applications.[10–12]

However, LIB performance is sensitive to certain factors in the operating environment, such as temperature,[13,14] pressure,[15] and vibration.[16] The ambient temperature has a considerable influence on the overall performance of LIBs, such as capacity, available power, charging/discharging efficiency, safety, and lifespan. The temperature sensitivity of LIBs stems primarily from the temperature sensitivity of the physical and chemical properties of the material. LIBs exhibits higher efficiency and a longer lifetime under ideal operational temperatures.[17] The thermal issue attracts attention to the precise battery thermal management system (BTMS) and current control to maintain the cell/module/pack temperature within the acceptable range (0–40°C). Considering the thermal safety and operational efficiency,[18,19] the cell body temperature should be maintained within 15°C–35°C. The system temperature deviation should be controlled below 5°C to enhance the lifespan and operational performance.[20–22]

BTMSs are proposed to satisfy these operating requirements, especially in extreme working conditions such as fast charging, severe high-temperature environments, or subzero cold zones.[23] Moreover, with higher requirements proposed for pure EVs, the energy density of LIB cells will be increased to extend the driving range. Fast charging technology will be widely employed to enhance long-term driving convenience.[24,25] Therefore, battery thermal management is crucial for solving emerging problems in the all-temperature area EV industry, such as severe lithium plating, overheating, and even thermal runaway (TR).[26,27] Moreover, more research is needed to enhance thermal management efficiency, thermal uniformity, and energy cost to cope with the future harsh requirements of BTMSs. Most existing reviews are organized for pure thermal management methods or structures.[28–30] This study provides a comprehensive overview and perspectives of LIB characteristics and thermal management strategies under all temperature areas and future requirements. As depicted in Figure 1, the basic idea behind this review is to give out the thermal performance, mechanisms, and strategies for the LIBs under all-temperature areas (1, low-temperature area [<0°C]; 2, normal temperature area [0°C–60°C]; 3 high-temperature area [>60°C]), from the performance, mechanism, and thermal management strategies levels.

LOW-TEMPERATURE AREA

Performance level

Subzero temperatures result in a negative impact on LIBs: (1) lower charge/discharge ability,[31] (2) less available energy and power capacity,[32] and (3) shorter lifespan.[23,33,34] The LIB output voltage decreases, causing lower energy density and power fading.[35] Consequently, the available energy loss under subzero temperatures reduces the EVs' driving mileages and available energy of the energy storage devices (ESDs). Moreover, the available power loss under subzero temperatures limits the quick acceleration and power frequency modulation of ESDs. Previous studies demonstrated that the 18650 $LiPF_6$ battery cell could only provide 5% and 1.25% of the power capacity (20°C) and energy capacity (20°C), respectively, under −40°C.[32] The driving range of the 2012 Nissan LEAF was reported to drop significantly from 138 miles under the ideal operational condition to 63 miles under −10°C. The usable charge/discharge capacity was calculated under low-temperature constant current charging/discharging tests.[32,36] Even in recent studies, with the development of battery technology, lithium-ion phosphate (LFP)/graphite-based battery cells could only provide available 70% and 60% capacities (refer to the room temperatures) under −10°C and −20°C, respectively. Furthermore, LIB rapidly degrade at subzero temperatures. You et al.[37] revealed that battery capacity fades nonlinearly after 500 cycles, under −5°C to 0.5°C cycling.

Under increasing charging rate requirements, lithium plating has more potential to occur, especially under a high state of charge (SOC) and subzero temperatures. Lithium plating facilitates gas generation, forming gas pockets on the electrodes, accelerating degradation, and even failure.[38]

Mechanism level

Low temperatures cause LIB deterioration (decreased ionic diffusivity, electrolyte conductivity, and anode lithium-ion diffusivity). In addition, the lithium-ion intercalation capacity of graphite decreases.[39,40] Moreover, the available capacity decreases with increasing internal resistance.[5,41–43] The charging/discharging capacity and efficiency are worse than those in typical applications. Furthermore, lithium evolution may occur inside the battery cell during high-current charging, harming the charging efficiency, lifespan, and safety.

Similarly, suppose that the LIB operates at subzero temperatures. The activity of the active material inside a battery is considerably limited. In this case, the internal resistance and polarization voltage increase.[44] Furthermore, the charging/discharging power and capacity are inevitably reduced, causing irreversible degradation of the LIB capacity and buried safety hazards. During the charging process, under an electric field applied by the charging equipment, lithium ions are extracted from the cathode material into the electrolyte, move to the anode, and enter the anode material composed of graphite to form an LC compound. Lithium ions cannot enter the anode in a timely manner to form an LC compound

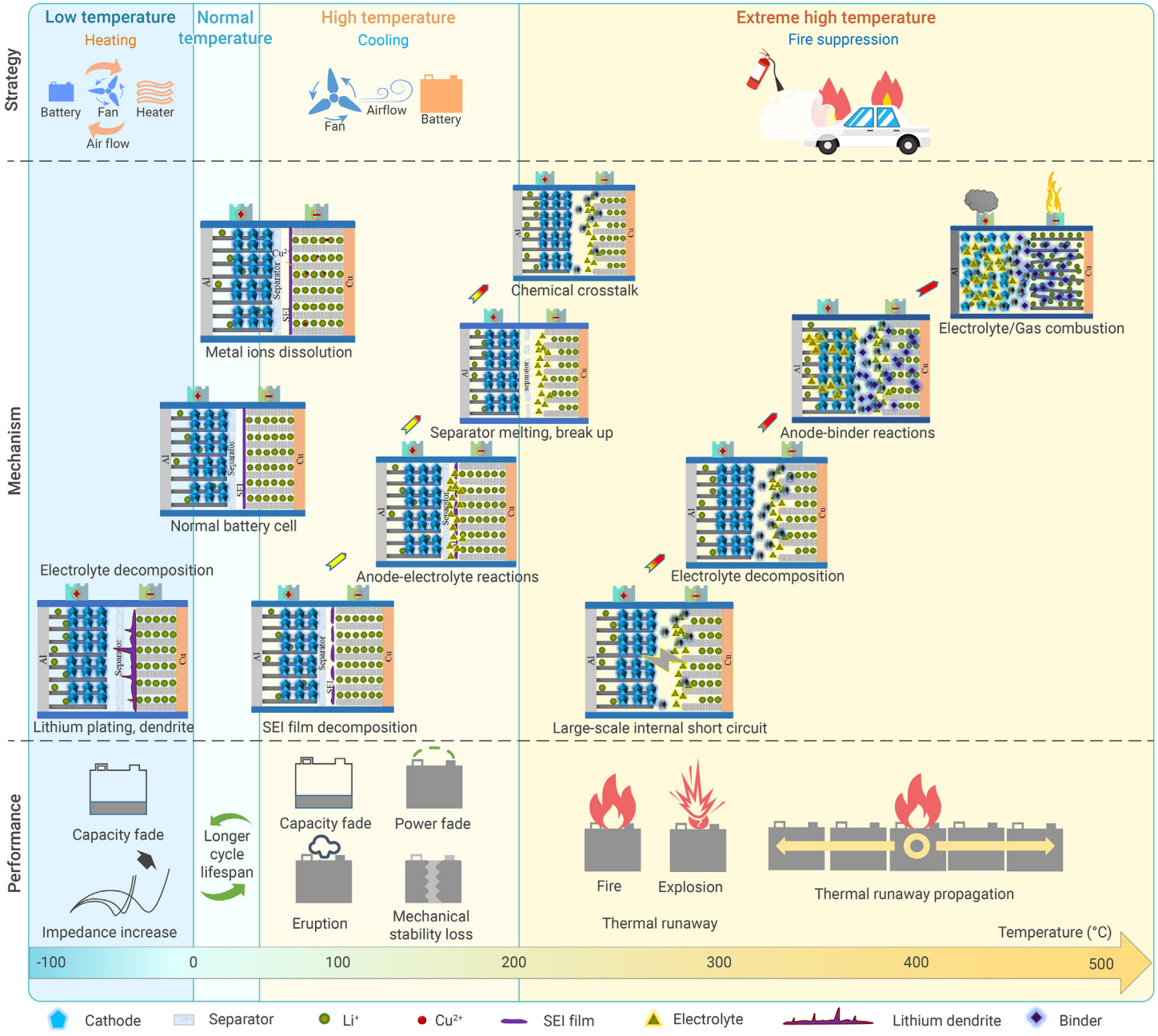

Figure 1. Performance, mechanism and strategies of lithium-ion batteries under an all-temperature area

while charging at high current rates and low temperatures. Lithium ions close to the negative electrode trap electrons, become metallic lithium, and aggregate to form lithium dendrites, which can grow. Piercing the diaphragm creates an internal short circuit.

Some existing research has proposed that the performance degradation of LIBs under subzero temperatures results from material property changes, which turns the stored energy into an unusable state.[45]

As shown in Figure 2, the intrinsic low-temperature degradation mechanism includes the following aspects.

(1) Limited electrolyte conductivity and increased viscosity affect the Li-ion transport rate between the two electrodes. Moreover, it has been reported that inadequate electrode activity results in limited performance. Electrode activity implies the combined effect of marginalized Li-ion transport through the solid-electrolyte interphase (SEI) film, increased charge-transfer resistance, intrinsic loss of ionic conductivity, and slower lithium-ion diffusivity within the anode materials.[46–48]

(2) The chemical composition and physical characteristics of the SEI film are also critical, such as the resistance to lithium intercalation, which depends on the salt-forming electrolyte, anode material quality, SEI formation mode, and temperature.[37,49,50] The SEI is the surface film on LIB electrodes, consisting of organic and inorganic components that maintain the electrolyte kinetically stable under an anode potential of less than 0.8 V. The SEI film thickness varies by approximately 0.5–80 nm, depending on the degree of anode graphitization.[51–53] However, the anodic film is less permissible for lithium-ion transportation at the electrolyte/electrode interphase, significantly increasing the battery impedance.[6,54,55]

(3) The diffusion of solid-state lithium ions decreases significantly, especially during the charging process (lithiation),[56] which contributes to the polarization. The graphite anode was more likely to be affected by lithium plating during charging.

(4) For the cathode material, the charge-transfer resistance increases by more than 200% compared with the normal charge-transfer resistance

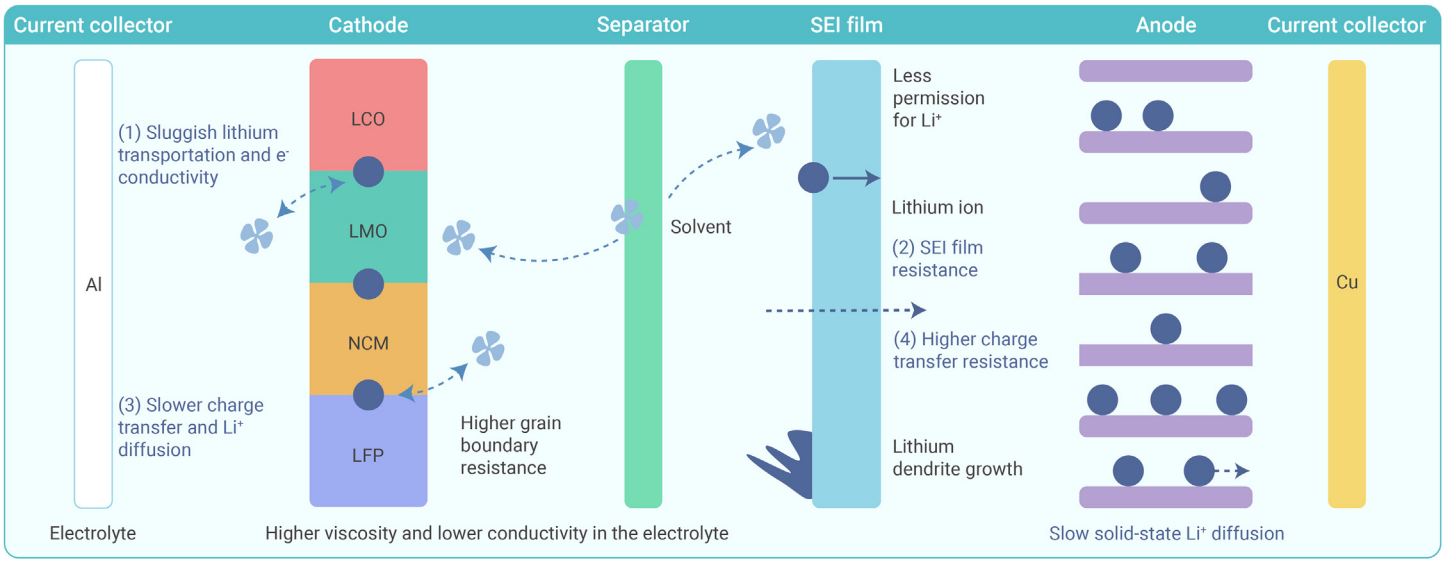

Figure 2. Battery degradation mechanisms under a subzero temperature area

during the discharging process (in the lithiated state).[57] Besides, high grain boundary resistance and slow solid-state diffusion contribute to the sluggish lithium transport and poor electronic conductivity of the cathode material.

Strategy level

Owing to the broad geographical applicability of automobiles, EVs inevitably operate in subzero temperature environments. Although a massive amount of heat is generated during the charging and discharging processes, the heat generated is insufficient for maintaining the cell within a suitable operating temperature range. Considering the limited charging and discharging performance in cold climates and high-altitude drone applications, preheating approaches are required to enhance battery performance at subzero temperatures.[58,59]

Low-temperature performance enhancement strategies can be summarized at the material, cell, and system levels.

Material level

Cathode modification. ***Decreasing particle size.*** As depicted in Figures 3A and 4I, decreasing the particle size provides a shorter diffusion path length for lithium ions and electrons and a broader electrolyte/electrode surface area for lithium-ion insertion and extraction, which results in enhanced electrochemical kinetics and low-temperature performance.[60,61] However, nanoparticles lead to more side reactions considering their high surface area and reactivity.[62] In addition, many binders are needed to glue these small particles together, inevitably decreasing the capacity. The low-temperature performance of other cathode materials such as $LiCoO_2$, $LiMn_2O_4$, and V_2O_5 has also been enhanced by decreasing the particle size.[63]

To avoid the nanoparticle electrode issues of reactive surfaces, limited particle contact, and retention of the merits of nanostructures, extensive studies have been conducted focusing on conductive coating materials and forming nanostructured electrodes.

Coating. As depicted in Figure 3B, similar to the carbon anode, electrolyte decomposition layers (EDL) still exist on the cathode surfaces.[71] The electrochemical behavior on cathode surfaces depends on the EDL properties.[72–74] Electrolyte component decomposition on the cathode is temperature sensitive[75] and depends on the electrolyte material.[73,76] Commercial cathode components are LiF, Li_2CO_3, $ROCO_2M$, $ROCO_2Li$, ROLi, MCO_3, MF_2 (M = transition metal), and polycarbonates,[72] respectively. Owing to its pronounced stability, EDL formation on the $LiFePO_4$ cathode differs from that on the Li_xMO_y host material (M = Ni, Mn).[77] Generally, the EDL thickness on $LiFePO_4$ is less than 5 nm in a 1 M $LiPF_6$ mixture of EC and DEC. An $LiFePO_4$ cathode coated with a carbonaceous material prevents undesirable reactions and enhances EDL stability.[78–81] Cathode coating significantly prevents contamination from HF and water.[72] Compared with the pristine $LiFePO_4$, a carbon-coated cathode capacity retention increases from 53.4% to 66.1% at −25°C.[64]

As Figures 3B and 4II show, an appropriately thin carbon coating is beneficial for balancing sufficient conductivity and Li^+ penetration,[82] especially for the superior electronic conductivity of carbon. Graphite is desirable for coating.[83,84] Uniform carbon coating for $LiFePO_4$ particles provides access for electrons from all directions to achieve low polarization.[85] Organic carbon pyrolysis produces a more uniform carbon film,[86] and increasing the porous carbon film surface area improves the conductivity.[87] However, excessive carbon significantly decreases the tap density of $LiFePO_4$ and generates some by-products, such as Fe_2P.[81,88] Therefore, the desirable carbon content in $LiFePO_4$/C is less than 5% wt.[89]

3D conduction network. As demonstrated in Figures 3G and 4III, to further enhance the conductivity and electrochemical characteristics, a three-dimensional (3D) conduction network was proposed.[90] Chang et al.[91] proposed a cathode material without any supplementary conduction agent. These results indicate that the prepared $LiFePO_4$ nanographite platelet) heterostructure enhances electron transport. Wu et al.[64] proposed 3D carbon-decorated $LiFePO_4$ nanocomposites with ultrahigh rate capability and enhanced subzero-temperature performance. Kim et al.[65] proposed a catalyst-assisted self-assembly approach to embed graphene onto $LiFePO_4$ as the cathode material, which exhibited superior cycling performance and rate capability.

Novel cathode material. To enhance the cycling performance under low temperatures.[92] As in Figure 4IV, Yoon et al.[66] investigated the subzero-temperature performance of $Li[Ni_xCo_yMn_{1-x-y}]O_2$ (NCM) cathodes with a 1.2 M EC-EMC (3:7 by volume) electrolyte. The results indicated that the low-temperature capacity of the NCM cathode was dependent on its chemical composition, which increased with increasing Ni content. Since high Ni content causes a high electrical conductivity, $Li[Ni_{0.85}Co_{0.075}Mn_{0.075}]O_2$ provides 127 mAh g^{-1} under a −20°C environment. Smart et al.[93] investigated the low-temperature performance of $Li_{1+x}(Co_{1/3}Ni_{1/3}Mn_{1/3})_{1-x}O_2$ cathode with a 1.2 M EC-EMC (20:80) electrolyte, which exhibited a 55% capacity retention at −40°C under high current rate discharging. The results indicated that a low ethylene carbonate content helped achieve a high discharge rate owing to its low viscosity and high ionic conductivity. Rui et al.[94] proved that an $Li_3V_2(PO_4)_3$/C (LVP/C)-based battery material provided a high discharging capacity of 108.1 mAh g^{-1} under −20°C environment. Its low-temperature performance was enhanced by the low activation energy of LVP (6.57 kJ mol^{-1}), causing more access to Li^+ extraction/intercalation in LVP.

Electrolyte modification. More researchers have recently focused on enhancing the electrolyte stability with effective SEI film formation. These studies can be summarized as follows:

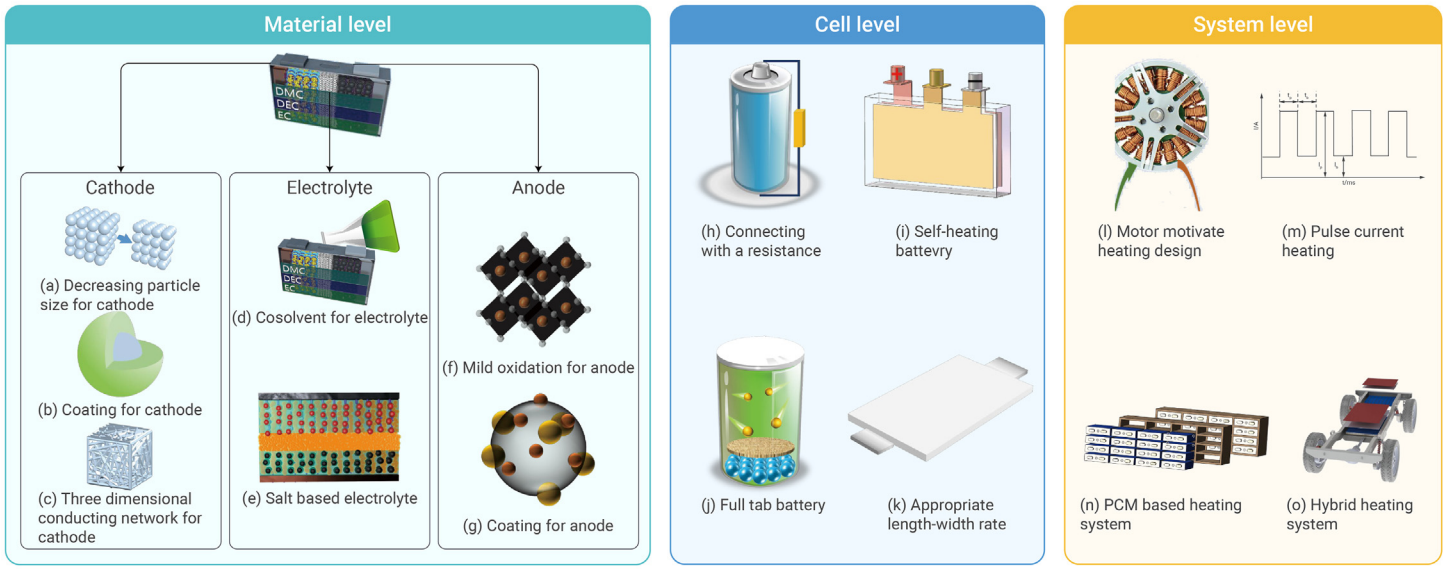

Figure 3. Strategies to enhance low-temperature performance of Li-ion batteries from different levels

(1) utilization of cosolvents with lower viscosity and lower freezing temperature, such as glymes, esters, and lactones.[95–98]
(2) changing the lithium salt $LiPF_6$ with new mixtures improved the charge transfer resistance and other characteristics of the SEI film.[99–104]
(3) formulation of new electrolyte additives to lower the freezing temperature.[105–109]
(4) novel electrolyte design to maintain the ionic conductivity within a desirable range.[110]
(5) LTO||LTO symmetric battery design to prevent high interface resistance owing to lithium-ion desolvation.[111,112]

The electrolyte determines the ionic mobility and participates in the reaction of SEI film formation on the anode.[113] The SEI film permits lithium-ion conduction, protects the electrodes, and prevents further electrolyte reduction, affecting the low-temperature performance and cyclic life.[47] Low-temperature performance can be achieved by improving the electrolyte conductivity and SEI stability at the electrolyte/electrode interface. The experimental results indicated that the electrolyte system can be optimized by adding suitable cosolvents and improving the Li salts.[106,114,115]

Adding cosolvent. The electrolyte solution conductivity drops rapidly in a low-temperature environment owing to the high freezing temperatures of conventional solvents (EC, DMC).[115] As depicted in Figure 3D, to reach a low freezing temperature but high conductivity under low temperatures, adding suitable cosolvents into the electrolyte has been proposed as a reliable method, which is selected considering some critical factors: (1) dielectric constant, (2) viscosity, (3) coordination behavior, (4) liquid range, and (5) pronounced chemical compatibility.

Salt selection. As Figures 3E and 4V demonstrate, Li salt selection also affects the lithium-ion conductivity and SEI stability, which is significant for enhancing the low-temperature performance.[116] $LiPF_6$ is a commonly utilized Li salt. However, it spontaneously decomposes into LiF and PF_5, thereby inducing structural changes and capacity fading. The selection of $LiPF_6$ with lithium tetrafluoroborate ($LiBF_4$) or lithium bis(oxalato)borate (LiBOB) enhances low-temperature performance because $LiBF_4$ or LiBOB-based electrolytes demonstrate low charge-transfer resistance.[117–119]

Anode modification. Limited Li diffusion in the electrodes and higher charge-transfer resistance at high charge/discharge current rates result in higher polarization and limited performance.[63]

The kinetic limitation of lithium-ion transfer at the electrode/electrolyte interface induces primary performance limitations at low temperatures. The electrochemical (faradic) reaction can be optimized by reducing R_{ct} and maintaining SEI stability.

Graphite is the most commonly used anode material for LIBs. However, its principal limitations are high R_{ct} values at the electrolyte-electrode interface, SEI instability, and reduced solid-state lithium diffusivity. Effective methods for improving the anode include the discussion of the following.[32,56,120]

Mild oxidation. As shown in Figures 3F and 4VI, mild oxidation of the graphite anode decreases the number of unsaturated carbon atoms at the edge planes, resulting in a smaller mean particle size.[121] Furthermore, this approach causes the formation of nanovoids, nanochannels, and chemically bonded SEI.[122] Consequently, the electrochemical impedance decreases, hindering the co-intercalation of solvated lithium ions and electrolyte decomposition. Mild oxidation can be achieved through thermal treatment or wet chemical oxidation.[67,123,124]

Mixing. Mildly oxidized graphite mixed with metal nanoparticles demonstrates enhanced low-temperature performance.[125] As Figure 4VII depicts, the oxidized graphite anodes mixed with 1% Cu and Sn in a 1 M $LiPF_6$ EC-DEC-DMC (1:1:1) electrolyte were proved to have the capacities of 130 mAh g^{-1} [122] and 94 mAh g^{-1} [68] at −30°C, respectively. The superior low-temperature performance resulted from the enhanced lithium-ion desolvation, increase in SEI conductivity, and internal conductivity of the metal-dispersed powder bulk electrode.[68]

Coating. Anode coating has been proven an alternative method to enhance electrochemical performance.[126] As shown in Figures 3G and 4VIII, the oxidized graphite anodes coated with 50 Å Cu and Sn layers in a 1 M $LiPF_6$ EC-DEC-DMC (1:1:1) electrolyte was tested to have the capacity of 103 mAh g^{-1} [123] and 152 mAh g^{-1} [68] at −30°C, respectively. Gao et al.[69] prepared a Cu-coated graphitic carbon anode via plating. The stable SEI suppresses the electrolyte decomposition (1 M $LiClO_4$ PC-DMC, 1:1 by volume) and achieves promising LIB performance at −60°C.[69] Therefore, the metal layers on the anode cause a remarkable decrease in R_{ct}, a stable SEI, and an increased lithium conductivity.[68,69,127]

Ag-Fe_2O_3/carbon nanofibers (CNFs) anode materials demonstrated pronounced electrochemical performances at −5°C due to their synergistic effects on the CNF matrix and the conducting Ag.[128] Li et al.[129] proposed Fe/Fe_3C-CNF materials with a high capacity of 250 mAh g^{-1} after 55 cycles at −5°C in a 1 M $LiPF_6$ EC-EMC-DMC (1:1:1 in volume) electrolyte.

Novel anode material. Raccichini et al.[70] synthesized a multi-layer graphene anode by combining microwave irradiation and ultrasonication in an ionic liquid. The low-temperature characteristics of multi-layer crystalline graphene (GRAL) and the commonly utilized graphite SLP30 in a 1 M $LiClO_4$ PC-DMC (1:1 by volume) electrolyte were compared. The results indicate that the GRAL capacity was higher than that of SLP30 at low temperatures. As shown in Figure 4IX, the low-temperature performance is enhanced owing to its high active surface area, which results in a higher anodic electrochemical reaction efficiency and improved lithium-ion diffusion kinetics.[130]

$Li_4Ti_5O_{12}$ is another promising low-temperature anode material with a high cycling stability. However, its sluggish lithium-ion and electron conductivities limit its electrochemical performance. Reducing the particle size of $Li_4Ti_5O_{12}$ and coating are typical methods to enhance electrochemical performance.[131,132] Yuan et al.[133] prepared nanosized rutile TiO_2 via a solegel approach, which

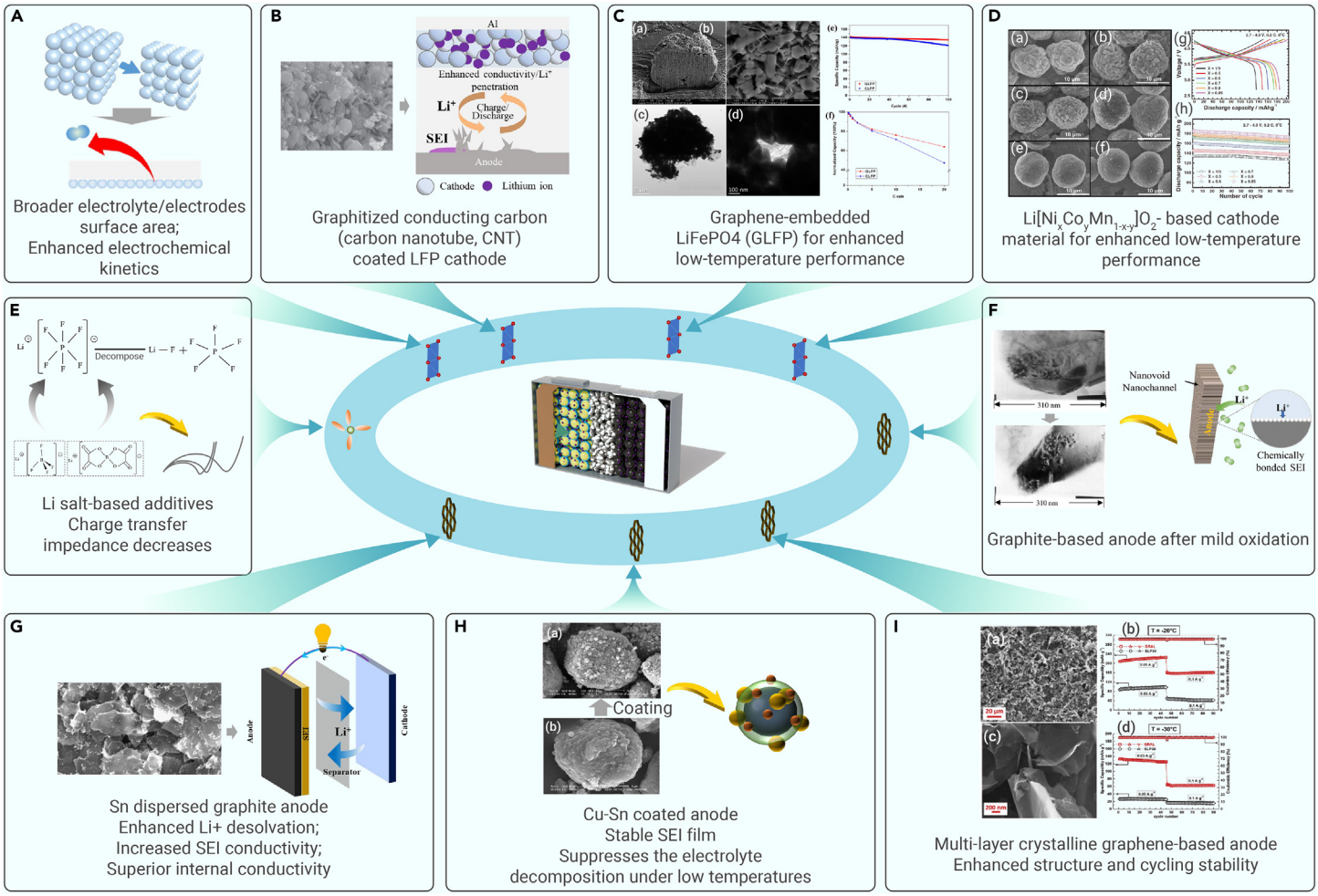

Figure 4. Schematic diagram of strategies to enhance low temperature performance (A) Decreasing cathode particles. (B) Coated cathode for enhanced low temperature performance (adapted from Wu et al.[64]). (C) Graphene embedded $LiFePO_4$ (GLFP).[65] (D) $Li[Ni_xCo_yMn_{1-x-y}]O_2$-based cathode material.[66] (E) Li salt-based additives. (F) Mild oxidized anode (adapted from Wu et al.[67]). (G) Mixed anode (adapted from Nobili et al.[68]). (H) Coated anode (adapted from Gao et al.[69]). (I) Multi-layer crystalline graphene-based anode.[70]

provides a capacity of 77 mAh g^{-1} at −40°C with a C/5 rate in a 1 M $LiClO_4$ PC-DMC (1:1 by volume) electrolyte.

Cell level

Connecting with a resistance. As depicted in Figure 3H, the battery cell can be connected to an external resistor, resulting in a closed loop. The current increased along the path inside the battery material. In addition, external resistance heats the battery surface. However, it is challenging to utilize and precisely control this heating approach in real applications, especially for massive battery cells in battery packs or energy storage stations, owing to local overheating and low heating efficiency.

Self-heating battery. As shown in Figure 3I, Wang et al.[39] proposed a self-heating battery cell by inserting an insulating polymer-coated metal foil. The switch between the activated and negative terminals can be closed to preheat the LIB to a low-temperature environment. Experimental results suggested that the battery temperature could be heated from −30°C to 0°C within 30 s through Ohmic heat generation. The switch was turned off until it reached 0°C, with 5.5% of the battery capacity consumed during the preheating process. Zhang et al.[40] concluded that nickel foil can accelerate spontaneous heat generation. There was a linear relationship between the inner temperature and the nickel foil resistance, which could be utilized as a temperature sensor to detect the internal temperature.

To enhance battery cell consistency, temperature gradients should be avoided.[134] However, a single nickel foil-based self-heating cell cannot ensure uniformity. Zhang et al.[40] proposed a self-heating cell with two or three pieces of nickel foil to address the issue. Moreover, the heating time was shortened, and the energy cost was reduced by 25%–30%. Compared with the slow heating rate issue of some external heating approaches, the self-heating rate reached 1°C–2°C/s. However, internal resistance heating efficiency may be limited by the electrothermal conversion efficiency.[58] Furthermore, considering the internal short-circuit-based mechanism and the complex operational conditions of EVs, the safety issue of changing the Li-ion battery cell's inner structure should be paid more attention to.[135,136]

Full tab battery. As demonstrated in Figure 3J, a full-tap battery has been proposed to achieve a trade-off between energy density and heat dissipation in recent years.[137] Conventional cylindrical batteries are commonly wound based on anode copper foil, cathode aluminum foil, and separator superposition. A pole lug was welded to both ends of the copper and aluminum foils for the outside electrode design. The winding length of a conventional 18650 cylindrical battery was 800 mm. To ensure low resistance, a long copper foil has high thickness and consistency requirements.

Taking the Tesla 4680 battery as an example, the full-tab battery converts the entire current collector into a tab, and the conductive path no longer depends on the tab. The current changes from the transverse transmission of the TS collector to the longitudinal transmission of the current collector. The entire conductive length decreased to 80 mm (battery height). The resistance is reduced from about 20 to 2 mΩ, calculated by the copper resistance formula. According to the ohmic heat theory, the internal resistance power cost can be reduced from 2 to 0.2 W.

Previous research has indicated that more tab numbers result in a less apparent internal temperature rise, and the current density of the battery tab increases, increasing the heat generation rate at the tab and causing a significant local temperature rise. The full-tab design effectively reduces the local current density and solves the thermal uniformity issue, which improves heat dissipation

and preheating efficiency. Therefore, the preheating efficiency, lifespan, and overall performance were enhanced when the batteries were heated using current.

Appropriate length-width rate for battery. As Figure 3K shows, large-scale battery cell schemes have been commonly used in recent years to achieve higher energy densities in battery systems. However, from the perspective of the current path, it is difficult to maintain thermal uniformity using a BTMS. In an inappropriate battery design, the current concentration around the tabs is different, which induces different heat accumulation issues, significantly affects the thermal uniformity and preheating rate, and can even cause overheating. In addition, a large cross-sectional area results in insufficient preheating efficiency. Therefore, an appropriate length-width ratio is important for battery design, especially in cold areas.

System level

As shown in Table S1, the preheating strategies utilized at the system level were evaluated and compared from various perspectives (heating rate, thermal consistency, safety, cost, and applicability).

Air heating. The air heating system flows hot air through the battery system.[22,138] The battery cells can be warmed by heat exchange between the airflow and battery surfaces.[18] Figure 5H shows that the air-cooling structure is designed based on air convection combined with heaters and control elements. Song et al.[139] found that the cell capacity was enhanced by 3.1% under a −3°C environment with a 5 kW heater-based air heating structure. Zhang et al.[140] utilized the EV's air conditioning system combined with pentadecane ($C_{15}H_{31}$) as the heat transfer medium under an ambient temperature lower than 0°C. The results demonstrated that the preheating efficiency, based on the phase change of pentadecane, was higher than that of the refrigerant. This strategy can be combined with an air-cooling system by combining the BTMS with heater control.

Liquid heating. Liquid heating is an approach for heating the cooling liquid to a specific temperature through the heating components of the vehicle, and the bump can be utilized for cycling the heated coolant in the battery module/pack.[141] To achieve all climate applications with low volume and weight costs, the liquid heating loop is commonly incorporated in the liquid cooling system. As shown in Figure 5F, a direct liquid heating system is proposed based on nonconductive transformer oil, a heating film, and a heat insulation layer. Nelson et al.[142] concluded that a silicone-oil-based liquid preheating system is effective for the cold start of LIBs. Wang et al.[143] inserted an L-shaped heating plate into the cell gap, and the fluid temperature of the heating plate evaporator was set to 40°C. Simulation results indicated that the preheating time of the battery module from −20°C to 0°C was controlled within 500 s.

PCM heating. Phase-change materials (PCMs) have received extensive attention owing to their latent heat without an extra power supply, which is a typical active heating/cooling approach.[144] As demonstrated in Figure 5E, latent heat can also be utilized for preheating under subzero temperatures. Zhong et al.[145] proposed a PCM-resistant wire-based BTMS with a fin for −20°C application. The central part's temperature of the battery module can be increased by 40°C within 300 s. Moreover, the fin structure can be utilized to prevent the thermal saturation prevention. Ling et al.[146] compared the heating effects of various composite PCMs. However, the proposed PCM did not have sufficient thermal conductivity, which resulted in a severe temperature deviation, uneven voltage distribution, and capacity loss. Therefore, to fulfill the requirements of fast charging and all-climate applications in next-generation BTMSs, PCM cannot achieve the desired thermal conductivity, volume, weight, latent heat density, and price.

PTC coupled heating. Positive temperature coefficient (PTC) resistance is a typical external heater based on the principle of Joule heat generation.[147] The metal heating wire is generally encapsulated in an insulating layer.[148] Li and Huang[149] proposed an aluminum plate scheme twinned with a PTC resistance wire for battery preheating. Fan et al.[150] conducted a simulation study to analyze the influential factors of a heating-plate-based BTMS. The results indicated that the heating efficiency increased with the coolant flow rate and coolant temperature. However, the maximum temperature exceeded 40°C when the inlet temperature was above 50°C. Chen et al.[33] conducted a thermal analysis to compare the preheating efficiency of two PTC-liquid heating systems under a −40°C environment. It was demonstrated that the preheating speed, thermal uniformity, and power consumption could be enhanced through appropriate structural design and preheating interval settings.

Alternating current heating. The feasibility of alternating current (AC) preheating in battery systems has been verified by setting alternative pulse currents through batteries.[151,152] Joule heat can be generated for preheating. Previous experimental results indicated that a high current amplitude was beneficial for temperature uniformity, and that the LIB performance did not degrade significantly.[153]

Zhang et al.[154] developed a sinusoidal AC heating structure with thermal insulation design. Repeated experimental results indicated that the preheating speed was positively correlated with the amplitude and heat insulation and was proven to have a negative correlation with frequency. Moreover, no significant capacity loss was observed after the tests. Furthermore, a lumped energy conservation model was proposed to predict the temperature rise for real-time preheating control.[134] Zhao et al.[155] compared the preheating efficiency of pulse heating and constant-current/voltage charging and found that the charging time could be shortened by 36 min (23.4%) and the charging capacity could be increased by 7.1% with pulse heating under the same operational conditions.

Ruan et al.[156] proposed an electrothermal coupling model-based internal heating system. A constant polarization voltage was controlled during heating to achieve a trade-off between the preheating interval and minor capacity loss. The heating efficiency of variable-frequency preheating was found to be consistent with that of constant-frequency heating. Therefore, constant-frequency heating can be selected for real applications, considering the feasibility of variable-frequency preheating.

A DC-DC converter can be used to amplify the output voltage to reach the desired charging voltage. Although external heating elements are not required for mutual pulse heating, their unique circuit and control elements increase the cost of the preheating system.[157]

Heating preservation. In summer, external high temperatures increase the LIB temperature. However, in severely low temperatures or winter, the internal temperature of the LIBs drops rapidly after parking outside for a long time, which affects the recharging, starting, and speed performance of the EV. Therefore, it is necessary to eliminate the impact of external high temperatures in summer or low temperatures in winter on the battery system through a thermal insulation design.[158] Insulation materials are employed to insulate and reduce the impact of external environmental factors.

A heat preservation system is commonly integrated with a BTMS to enhance cooling/heating efficiency, and energy consumption can also be controlled.

NORMAL TEMPERATURE AREA

Performance level

Ambient temperature directly affects the activity and conductivity of the electrode material, the insertion and deintercalation of lithium ions on the electrode, and the lithium-ion permeability of the separator. Furthermore, ambient and internal temperatures affect the electrochemical reactions inside the battery cell. Therefore, LIBs have a normal operating temperature range without severe heat generation.

As the temperature increases within this range, the activity of the internal active materials is enhanced, and the charging/discharging voltage, efficiency, and capacity of the battery increase accordingly, resulting in a corresponding reduction in the internal resistance. However, as Figure 6 depicts, the internal side reactions accelerated when the battery temperature exceeded a specific range. These side reactions consume lithium ions, solvents, and electrolytes, degrading the battery performance. Previous studies demonstrated that LIB cycle life is significantly reduced when the battery works above 60°C. This phenomenon is more evident during high-rate charging and discharging, and can lead to accidents.

The calendar lifespan of EVs and hybrid electric vehicles was defined as 10 or 15 years.[159] However, the LIB temperature can be easily elevated to a relatively higher value, such as 40°C, which accelerates the ageing process, resulting in the loss of the retention capacity.

LIB performance is also influenced by temperature rise and deviation resulting from heat generation, ambient temperature, and different degrees of electrochemical reactions that occur at all times.

Existing studies have proven that the heat-generating rate of LIBs has a quadratic relationship with the charging/discharging current. At high

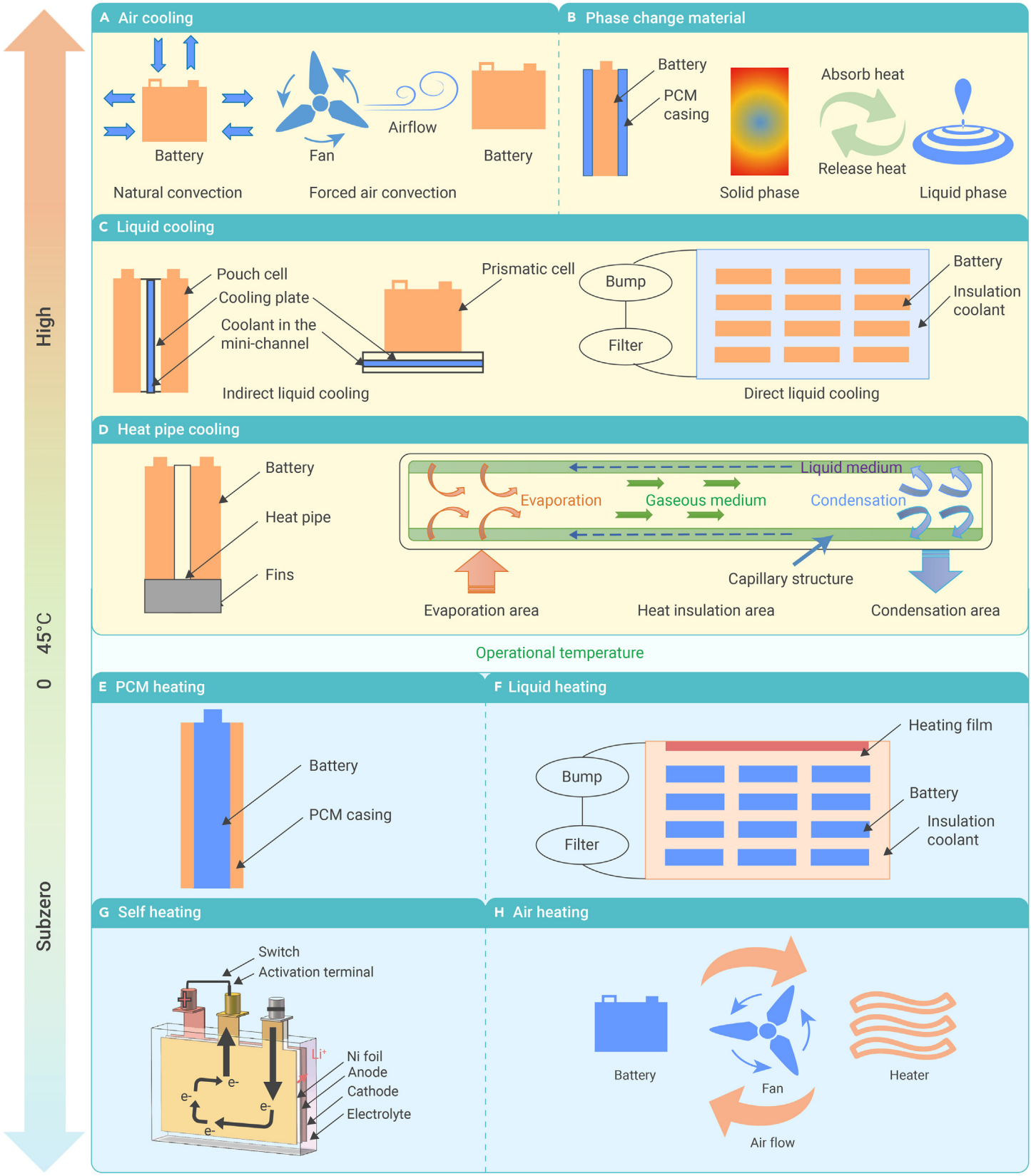

Figure 5. Scheme of thermal management strategies (A) Air cooling, (B) liquid cooling, (C) phase change material cooling, (D) heat pipe cooling, (E) PCM heating, (F) self-heating battery, (G) liquid heating, and (H) air heating.

ambient temperatures or during high-rate charging/discharging, the corresponding heat dissipation methods should be utilized to control the increasing temperature. Otherwise the cell will be overheated, causing performance degradation, a shortened lifespan, or even a dangerous state of TR.

Mechanism level

Almost all main/side reactions are related to temperature. The side reaction rate increases at high temperatures. Moreover, self-heating and thermal accidents can occur when the temperature exceeds a certain threshold. At subzero temperatures, the polarization increases owing to the increase in internal

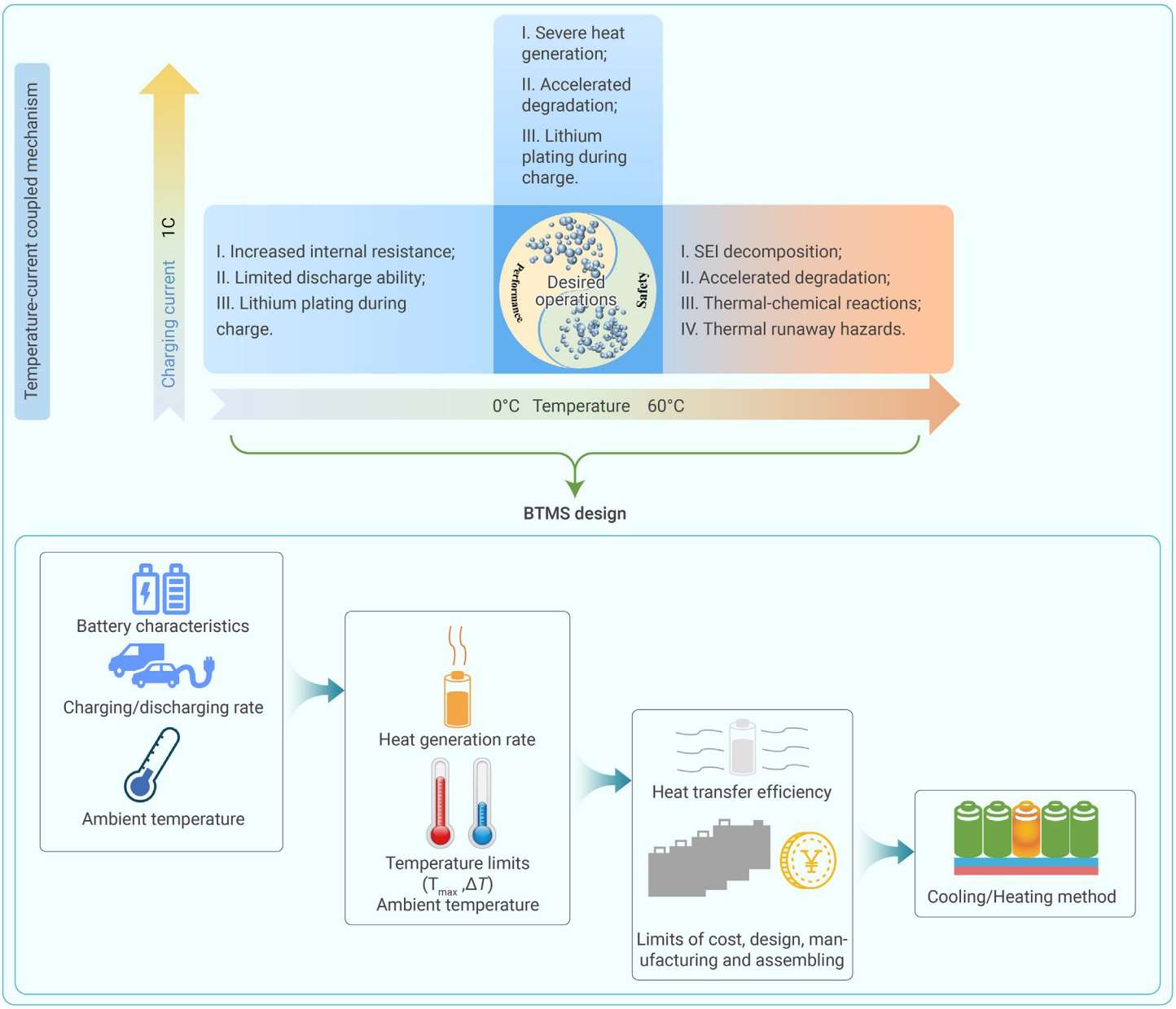

Figure 6. Schematic diagram of the temperature-current coupled mechanism and BTMS design for lithium-ion batteries

resistance, causing other side reactions. Charging at low temperatures triggers lithium deposition, accelerates degradation, and causes safety issues. Furthermore, material embrittlement under subzero temperatures limits battery cycle life. Therefore, maintaining battery temperature within the above-mentioned temperature range (15°C–35°C) is significant for the overall performance and cycle life.

In the normal temperature range, batteries exhibit desirable operational efficiency. The lithium ions were smoothly inserted and extracted from the anode. Only the degradation (loss of active material/lithium inventory/conductivity) and heat generation mechanisms during the cycling process affect the battery thermal performance, rather than the other side reactions.[160] The heat generation mechanism under the normal temperature range is discussed in the supplemental information.

Strategy level

Under normal temperature conditions, LIBs do not require heat or fire suppression. However, heat generation during conventional charging/discharging cannot be neglected because it may exceed the threshold of some side reactions. The cooling component of the BTMS is used to prevent overheating. Because of the characteristics of the battery system, thermal consistency should be maintained to guarantee the desired performance and cycle life of the battery system.[161]

According to the heat transfer media, the commonly used cooling methods in the EV market can be divided into three main categories (1) air cooling,[162] (2) liquid cooling,[163] and (3) PCM cooling.[164] In addition to being distinguished based on the cooling medium, cooling is often classified as active or passive based on whether additional energy is consumed in the cooling process. Cooling efficiency is mainly characterized by the convective heat transfer coefficient. Generally, the convective heat transfer coefficient required by the BTMS is determined by the operational environment of the EV, LIB characteristics, and other factors, such as weight, volume, and cost.

As shown in Figure 6, the selection of cooling approaches included the following steps: (1) confirmation of cooling system objectives, (2) calculation of heat generation power, (3) establishment of a battery model, (4) thermal fluid dynamic simulation analysis, (5) convection coefficient analysis, and (6) cooling method selection.

Table S2 summarizes the critical technical standards for the typical cooling strategies for battery systems. A detailed discussion of the specific cooling approaches is provided in the supplemental information.

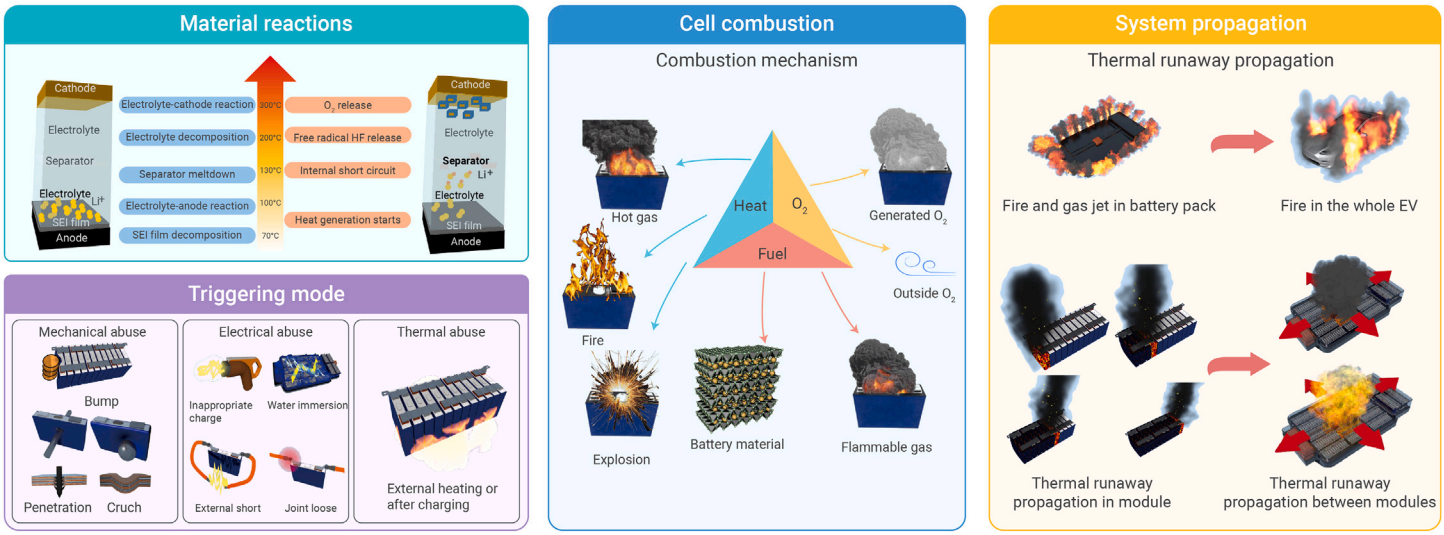

Figure 7. Thermal runaway scheme of lithium-ion under extreme high temperatures (Triggering mode; Mechanism; Fire resources; Thermal runaway propagation paths).

HIGH-TEMPERATURE AREA

Performance level

Fire behavior. As demonstrated in Figure 1, when the battery temperature exceeds 60°C, high temperature triggers SEI film decomposition and self-heating. Massive heat is released under high-temperature areas or abuse operations owing to chemical reactions and ISC, and the battery temperature rises rapidly.[165] Simultaneously, the safety valve opens when the internal pressure reaches a threshold, or the battery casing swells and breaks. Furthermore, aerosols and flammable gases are ejected at high speeds and temperatures.[166] These flammable materials tend to ignite in air when the air-fuel mixture ratio is within the flammability range, resulting in combustion.[167]

Ping et al.[168] carried out a full-scale burning test for a 50 Ah LFP/graphite battery pack. The combustion behavior of a 100% SOC pack can be divided into several stages: (1) battery expansion, (2) jet flame, (3) stable combustion, (4) second flame jet, (5) stable combustion, (6) third flame jet, (7) stable combustion, and (8) abatement and extinguishment.

Thermal runaway propagation. An increasing number of battery cells are tightly connected in series or parallel to meet the demand for capacity and power in EV battery packs and energy storage stations.[169] As in the Tesla Model S, the battery pack is equipped with seven thousand 18650-format LIBs, and the total energy reaches 85 kWh. However, the total heat released from the battery module is not the sum of the combustion energies of each cell. The proportion is proven to be 1.26.[170] Therefore, TR and fire may propagate throughout the module/pack. A TR fire promotes the combustion of other cells to a higher fire intensity, resulting in catastrophic disaster.[171]

Generally, the thermal runaway propagation (TRP) from the center cell through the entire pack is faster than TR initiation from the corner.[172] In addition, the electrical connection mode influences the TRP characteristics within a battery module.[173] Ten 18650-format cylindrical LIBs were connected as an equilateral triangle module, and the center cell was penetrated to trigger TRP. The results indicated that the parallel configuration resulted in an external short circuit with other cells. The surrounding cells were triggered in the parallel-connection mode rather than in the series-connection mode.

The battery format (cylindrical/prismatic/pouch) also affects the TR dynamics. Owing to the limited physical contact between neighboring cylindrical battery cells, the cylindrical battery module was less prone to TRP than the pouch cell module.[173–175] Heat transfer between neighboring pouch cells was identified as the primary driving force for TRP.[176]

There are three heat transfer paths within the battery module during the TRP process: (1) heat conduction through the battery shells, (2) heat conduction through the pole connectors, and (3) convection and radiation from the flame to the battery cells. Feng et al.[177] concluded that heat was mainly transferred through the shell, which mainly depended on the TRP behavior, and was approximately ten times higher than the heat transfer through the pole connectors. The heat that triggers the neighboring cell for TRP is less than 12% of the total heat released during the TR process. The thermal resistance between the neighboring cells and the triggering methods determine the TRP characteristics within a battery module.[177–179] However, flame impingement determines the fire propagation within a battery module. The flame and convection/radiation from the flame significantly affect the temperature of the LIB in contact.[180]

Mechanism level

The self-heat generation of LIBs occurs in high-temperature environments or under electrical/mechanical abuse. When the accumulated heat from the exothermic reactions cannot be dissipated into the environment, the battery temperature increases continually. Furthermore, the impervious SEI film breaks down and dissolves, exposing the anode surface to electrolytic corrosion accompanied by irreversible lithium loss. Moreover, SEI film dissolution disturbs the physical balance state of the SEI metastable organic components, which form a more stable inorganic material such as lithium carbonate.[181] The ionic conductivity and permeability of the SEI film gradually decrease as the inorganic carbonate ratio increases, causing a significant reduction in the LIB energy capacity and output power.[182,183]

As shown schematically in Figure 7, the meltdown process of the cell consisted of three steps. The first step is the electrochemical breakdown of the anode SEI film, which starts at around 70°C.[184–186] Besides, the intercalated lithium reacts with $(CH_2OCO_2Li)_2$. When the heat is insufficiently dissipated from the LIB during this step, the governing electrochemical reaction becomes self-sustained.

Without protection from the SEI film, the following reaction is between the electrolyte and carbon anode.[187] Furthermore, if the self-heat generation rate exceeds 0.2 °C/min, the defined TR phenomenon occurs.[188,189] The melting temperatures of the PE, PP, and ceramic-coated separators are around 135°C, 166°C, and 200°C, respectively.[190] The second step of the separator meltdown process commonly starts at around 130°C, with the symbol of exothermic activity on the cathode. In this step, the self-heat generation rate of the cell increased to approximately 5°C/min. The cathode and anode layers are in direct contact with each other, resulting in a large-scale internal short circuit,[191] which is a critical inducement of TR. The energy released during the TR process is approximately equal to the energy stored in the battery cell.[192] However, LIB TR can also be triggered without ISC, and may be induced by chemical crosstalk.[193]

The final step began at temperatures greater than 200°C. Oxygen is rapidly released during the cathode decomposition,[193] and the self-heat generating rate of the cell increases to higher than 10°C/min with the decomposition of the cathode, the oxidization/decomposition of the electrolyte. The temperature increases to 100°C/min in some severe meltdown processes,[184,194–196] releasing carbon dioxide, fluoride gas, and hydrocarbons.[197–200]

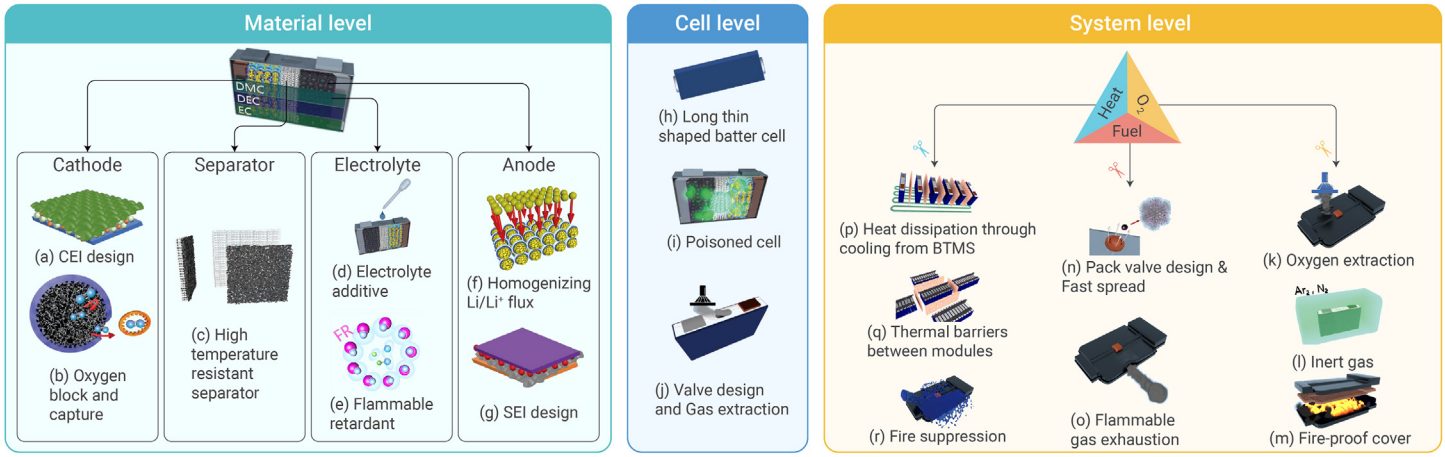

Figure 8. Thermal runaway mitigation strategies for Li-ion batteries from different levels[205]

The driving temperature for the exothermic TR reaction depends on the chemical components and the SOC.[201,202] Generally speaking, with a higher voltage or SOC value, the onset temperature for the LIBs, TR is lower. However, even for specific battery types with the same chemical components, the onset temperature varies with load history and abuse events.[184,203]

Strategy level

As summarized in the previous analysis, heat and flammable gas generation directly determine the TR hazard. Therefore, battery system safety can be enhanced through the following approaches: (1) preventing or alleviating heat and gas generation and (2) managing heat and gas generation. Safer battery cells can be fabricated by modifying the materials, inner structures, or safety devices. The incorporated safety equipment can be classified as a safety vent, current interrupt device, shutdown separator, detection component, BMS, BTMS, or fire suppression device.[204–206] Furthermore, from a thermal management perspective, battery system safety can be enhanced by equipping an efficient BTMS and fire suppression devices.

Material level

Based on a previous study on the TR mechanism, the quantified TR mitigation target was to increase the self-heat generation temperature (T1) and TR onset temperature (T2) to inhibit TR triggering and to decrease the maximum temperature (T3), which decreases the heat released during the TR process.[205]

Cathode modification. ***Oxygen block and capture.*** In addition to the flammable gases generated during the TR process, oxygen released from the cathode has been proven to be a significant TR factor, resulting from the cathode-anode chemical crosstalk.[193] Therefore, as demonstrated in Figure 8B, a cathode coating is proposed as an intuitive method to block the release pathway for O_2.[207,208] However, a specific solution is needed for the cathode coating to immediately capture the active O_2 release with reliable electrical performance and cycle life. Feng et al.[205] proposed replacing the polycrystalline secondary structure with a single-crystal morphology to reduce the O_2 release surface area.

Separator modification. As depicted in Figures 8C and 9I, to postpone the occurrence of large-scale ISC, a high-temperature resistance separator should be designed against shrinkage in a hot environment,[209] such as by selecting a thermal-resistant base material and coating with ceramic or other materials that do not break up under high temperatures. Rahman et al.[210] prepared a separator coated with boron nitride nanotubes. Results indicated that the proposed separator enhances the thermal stability up to 150°C without blocking the lithium-ion diffusion.

Anode modification. The coated layer on the anode surface also remained intact during cycling, preventing lithium metal deposition on the anode-electrolyte interphase. Therefore, there is no massive irreversible lithium plating on the anode to induce large-scale ISC. As depicted in Figure 9II, Friesen et al.[212] prepared an anode material coated with Al_2O_3, which suppressed Li dendrite growth and demonstrated no deterioration in the thermal and mechanical safety behavior, despite thick Li deposition on the anode surface.

Electrolyte modification. ***Electrolyte selection.*** As Figure 8D shows, a more stable SEI film formation is required to postpone the self-heat generation state, which can be achieved by adding electrolyte additives.[214] Ma et al.[215] investigated the impact of electrolyte additives (vinylene carbonate [VC], fluoroethylene carbonate, and vinyl ethylene carbonate) on electrode/electrolyte reactions. Results indicated that adding VC decreases the lithiated graphite-electrolyte reactivity below about 200°C. Liu et al.[216] proved that electrolyte additives enhance SEI uniformity and suppress dendrite growth.

As depicted in Figures 8E and 9III, flame-retardant electrolyte additives have also been considered as alternative mitigation approaches in recent years. Hou et al.[217] proved that flame-retardant fluorinated electrolytes reduce heat release during the TR process, which guides safer LIB design through appropriate electrolyte design.

Cathode-electrolyte interphase design. To pursue higher energy density, the nickel content in the cathode material has been increased in recent years.[218] As Figures 8A and 9IV demonstrate, *in situ* robust cathode-electrolyte interphase formation and control are considered the promising cathode enhancement strategy to address the aggressive thermal reaction by forming a protective layer on the cathode, which has been investigated through appropriate electrolyte selection (conventional carbonate-based electrolyte, fluorinated electrolyte, concentrated electrolytes, or solid-state electrolyte) and adding additives.[211] Besides, the operational environment, such as temperature and pressure, should be precisely controlled during pristine and post-cycling to achieve a stable and uniform interphase formation.

Cell level

Blade battery cell. As shown in Figure 8H, a blade battery cell is proposed with a trend of higher system energy density and larger scale. Zhang et al.[219] observed the TR front phenomenon in a long-shaped battery, which propagated at a moving rate. In real applications, an ISC failure after lithium planting or a defect inside it generally triggers TR accidents. A severe TRP temperature increase within a cell or battery system can be detected by a BMS and stopped by fire-distinguishing devices. In addition, thin, long battery cells were designed with fewer electrode layers. The energy released from the ISC is less than that from conventional batteries, especially when the LIB is penetrated/squeezed/triggered by a defeat ISC/partially overheated. The heat that propagates to other areas or neighboring cells is less and can even be cooled with proper heat dissipation or other mitigation countermeasures. Therefore, a long battery design is beneficial for TRP mitigation.

Self-poisoned battery cell. As Figure 8I shows, to reduce the heat released during the TR process, neutralizing the oxidant and reductant is considered a promising strategy for mild reactions,[220] which can be achieved using the following methods.

(1) application of thermoresponsive materials to block the cathode-anode contact.[221,222]

(2) structural design of current collector to isolate damaged area.[223]

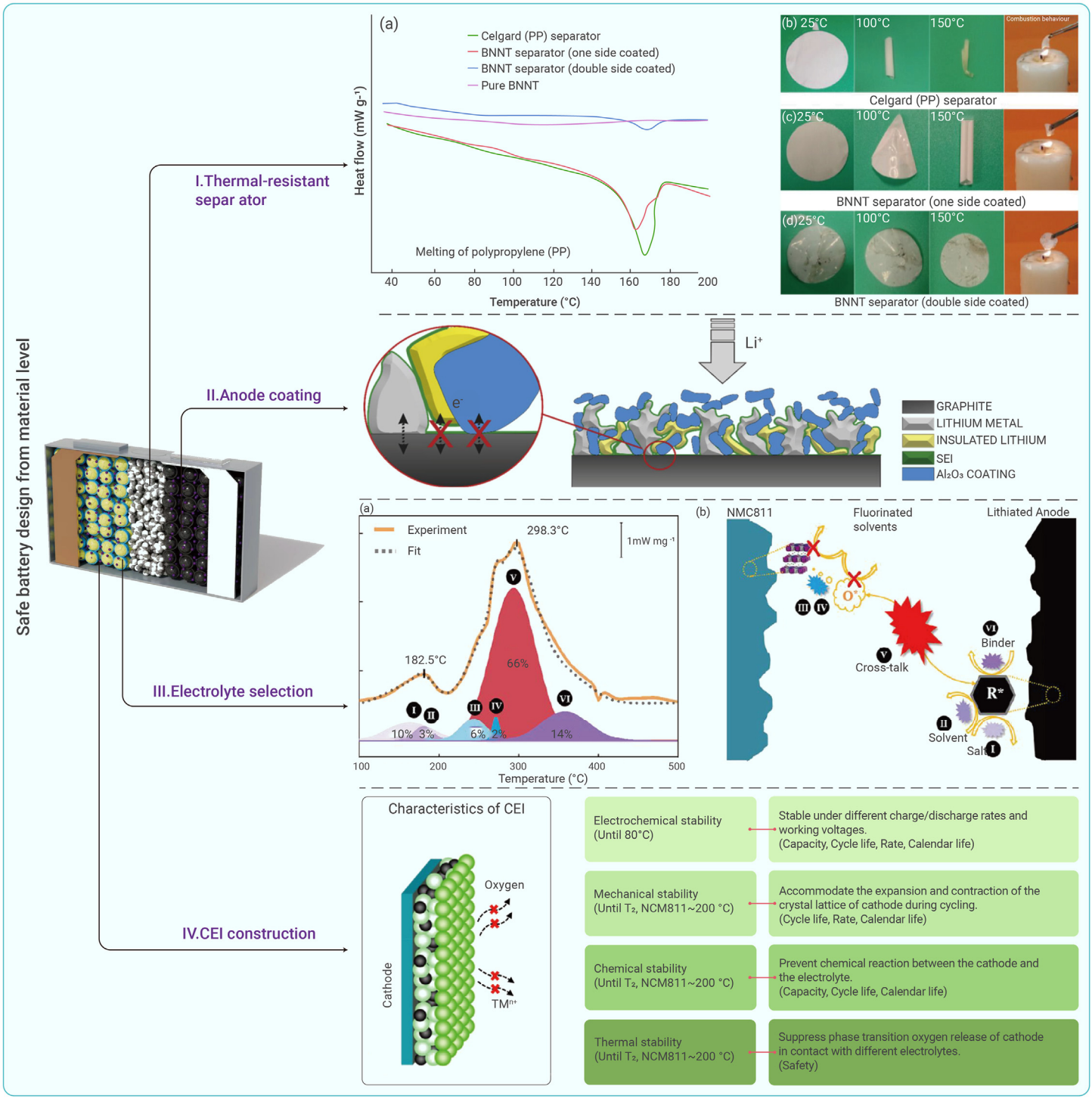

Figure 9. Schematic diagram of safe battery material design (I) Cathode-electrolyte interphase [CEI] design.[211] (II) Thermal-resistant separator.[210] (III) Al_2O_3-coated anode,[212] and (IV) flame-retardant electrolyte.[213]

Liu et al.[224] prepared an electrospun separator with a core-shell structure containing a flame-retardant liquid within the microfibers. Lai et al.[225] utilized a poison agent to mitigate the TR process, and results indicated that the energy release was significantly reduced and the maximum temperature was decreased by more than 300°C. However, it is necessary to guarantee the normal operation of LIBs. A reliable packaging material is urgently needed for the poisoning material to prevent the long-term corrosive effect from the electrolyte, the suppression behavior due to the LIB "breathing effect." In addition, avoiding internal structural changes in ISC is critical for safety during long-term cycling.

Safety valve design and gas extraction. As depicted in Figure 8J, proper design of the battery vent valve is significant for controlling the rupture moment at an appropriate temperature level, which might help diminish the venting damage and TRP.[226]

System level

Detection devices. To avoid abnormal temperature environments or electrical loads, a BMS can be incorporated with a battery system for battery state monitoring.[227] With timely detection and reporting of abnormal battery states, it is helpful to avoid overheating,[228] overcharging, or overdischarging.[229] In addition, BMSs utilize effective methods (such as timely discharge) to alleviate abuse conditions, even preventing TRP disasters.[230] However, it is challenging for BMSs to detect ISC, which results from various factors, including manufacturing.[179]

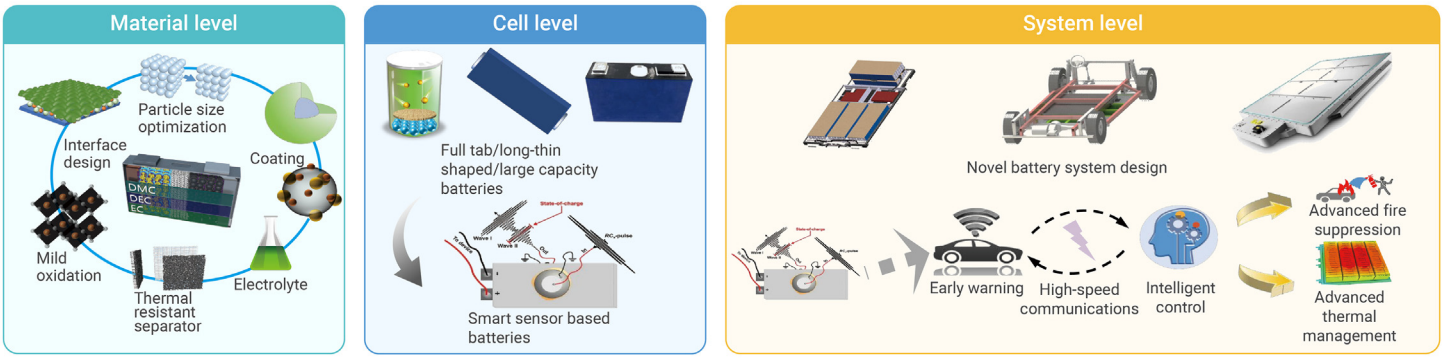

Figure 10. Future strategies to enhance the all-temperature area performance and safety

Apart from the temperature, current, and voltage detection of LIBs,[230] gas and smoke detection[231] during the TRP process is also significant, especially within a battery system with a progressively larger size and higher energy density.[232]

TR propagation mitigation design for oxygen. Oxygen extraction. As shown in Figure 8K, oxygen extraction using a mini-bump may be helpful for TR fire mitigation, even if oxygen is generated from the cathode during the TR process. Continuous gas extraction cannot provide sufficient oxygen for the flame reaction, and TR propagation may stop.

Inertia gas environment. As Figure 8L demonstrates, wrapping the battery system in an inert gas environment helps suppress the TR fire propagation.[233,234] Diluting the flammable gases and oxygen to a lean level might eliminate the flame.

Fire-proof cover. As shown in Figure 8M, attaching a thick fireproof cover on top of the battery system prevents fire from spreading. In addition, when a fireproof cover is designed with reliable sealing ability, oxygen can be decreased to a certain level with continuous consumption during the flame reaction. Furthermore, to protect passengers, a fireproof cover is essential to insulate the battery system from the cabins.

TR propagation mitigation design for fuel. Pack valve design and fast spread. As depicted in Figure 8N, when the pressure resistivity of the pack vent valve is lower than that of the pack wrap, expected venting occurs, and gases emerge from the vent valve. The gases can vent spontaneously once the pressure requirements are satisfied.

Flammable gas exhausting. As shown in Figure 8O, the gases inside the battery system can be extracted from the pack by using a bump with an appropriate gas channel design. Therefore, without sufficient flammable gases and oxygen, the TR fire cannot spread to the LIB even if the first cell is fired during the TR process.

TR propagation mitigation design for heat. Cooing. As Figure 8P shows, the heat conduction and dissipation efficiency of the commonly utilized liquid cooling system can be reinforced to prevent TR propagation.[206] Moreover, PCM barriers can be combined to absorb the massive heat during the TR process.[27] To cope with the dilemma of high energy density and thermal safety; higher heat capacity and composite PCM barriers are considered promising solutions for TR propagation prevention in high-nickel ternary material battery systems.

Heat insulation. The heat transfer pathway through the surfaces between adjacent cells is the primary heat source, as shown in Figure 8Q. Setting thermal insulation barriers between neighboring cells and battery modules is a cost-effective method for mitigating TRP.

The proposed heat-insulation materials include ceramic plates, rock wool panels, glass fibers, perlite, calcium silicates, silica aerogel,[192] Al extrusion,[192] and graphite composite sheets. However, thermal barriers utilized for TRP prevention should be thermal resistant (>600°C) and have low thermal conductivity (<0.1 $W\,m^{-1}\,K^{-1}$).[235] Besides, a reliable thermal barrier should maintain the heat insulation area under high-temperature burning and fire impact.[236]

Fire extinguishing. As shown in Figure 8R, the typical approaches to fire suppression can be divided into (1) isolation, (2) smothering, (3) cooling, and (4) chemical suppression. Unlike typical fires, some battery fires result from direct reactions between the components. These reactions do not require external oxygen.

A detailed discussion of the fire extinguishing studies is provided in the supplemental information. Table S3 compares the characteristics and critical standards of commonly utilized extinguishing agents for battery fire disasters that guide fire suppression designs for battery systems. Table S4 summarizes the TR/TRP mitigation strategies for high-temperature hazards at the material, cell, and system levels.

CONCLUSION

As the primary obstacle for large-scale LIB applications, thermal issues remain challenging to address, especially for all-climate applications and severe operations, such as fast charging. This study comprehensively reviews the thermo-electric characteristics and mechanisms in all climate areas. To enhance performance and ensure safety in all-temperature areas, advanced thermal management and fire suppression strategies for LIBs have been introduced from the perspectives of subzero, normal, and high temperatures. In addition, as demonstrated in Figure 10, to further address the all-temperature area thermal issues, promising future strategies are provided from the perspectives of the material, cell, and system levels, which include novel material preparation, battery cell design, battery thermal management, warning, and fire suppression technologies (provided in the supplemental information).

REFERENCES

1. Sun, J., Chen, S., Shen, K., et al. (2022). Liquid cooling system optimization for a cell-to-pack battery module under fast charging. Int. J. Energy Res. ***46***, 12241–12253.
2. Wang, H., Chen, S., and Du, Z. (2021). Side plate-based cell-to-pack LiNi0.5Co0.2Mn0.3O2 lithium battery module design with internal temperature acquisition and precise thermal modeling. Int. J. Energy Res. ***45***, 21254–21263.
3. Chen, S., Zhang, G., Zhu, J., et al. (2022). Multi-objective optimization design and experimental investigation for a parallel liquid cooling-based Lithium-ion battery module under fast charging. Appl. Therm. Eng. ***211***, 118503.
4. Roveda, A.C., Comin, M., Caires, A.R.L., et al. (2016). Thermal stability enhancement of biodiesel induced by a synergistic effect between conventional antioxidants and an alternative additive. Energy ***109***, 260–265.
5. Wang, X., Wei, X., Zhu, J., et al. (2021). A review of modeling, acquisition, and application of lithium-ion battery impedance for onboard battery management. eTransportation ***7***, 100093.
6. Zhang, S.S., Xu, K., and Jow, T.R. (2004). Electrochemical impedance study on the low temperature of Li-ion batteries. Electrochim. Acta ***49***, 1057–1061.
7. Fuller, T.F., Doyle, M., and Newman, J. (1994). Simulation and optimization of the dual lithium ion insertion cell. J. Electrochem. Soc. ***141***, 1–10.
8. Feng, X., Merla, Y., Weng, C., et al. (2020). A reliable approach of differentiating discrete sampled-data for battery diagnosis. eTransportation ***3***, 100051.
9. Han, X., Lu, L., Zheng, Y., et al. (2019). A review on the key issues of the lithium ion battery degradation among the whole life cycle. eTransportation ***1***, 100005.
10. Chen, S., Bao, N., Peng, X., et al. (2020). A Thermal Design and Experimental Investigation for the Fast Charging Process of a Lithium-Ion Battery Module With Liquid Cooling. J. Electrochem. Energy Convers. Storage ***17***, 021109.
11. Tomaszewska, A., Chu, Z., Feng, X., et al. (2019). Lithium-ion battery fast charging: A review. eTransportation ***1***, 100011.
12. Tanim, T.R., Dufek, E.J., Walker, L.K., et al. (2020). Advanced diagnostics to evaluate heterogeneity in lithium-ion battery modules. eTransportation ***3***, 100045.
13. Wang, Q., Jiang, B., Li, B., et al. (2016). A critical review of thermal management models and solutions of lithium-ion batteries for the development of pure electric vehicles. Renew. Sustain. Energy Rev. ***64***, 106–128.

14. Yi, Y., Xia, C., Feng, C., et al. (2023). Digital twin-long short-term memory (LSTM) neural network based real-time temperature prediction and degradation model analysis for lithium-ion battery. J. Energy Storage ***64***, 107203.
15. Jamal-Abad, M.T., Zamzamian, A., and Dehghan, M. (2013). Experimental studies on the heat transfer and pressure drop characteristics of Cu-water and Al-water nanofluids in a spiral coil. Exp. Therm. Fluid Sci. ***47***, 206–212.
16. Zhang, Y., Chen, S., Shahin, M.E., et al. (2020). Multi-objective optimization of lithium-ion battery pack casing for electric vehicles: Key role of materials design and their influence. Int. J. Energy Res. ***44***, 9414–9437.
17. Bandhauer, T.M., Garimella, S., and Fuller, T.F. (2011). A critical review of thermal issues in lithium-ion batteries. J. Electrochem. Soc. ***158***, R1.
18. Jaguemont, J., and Van Mierlo, J. (2020). A comprehensive review of future thermal management systems for battery-electrified vehicles. J. Energy Storage ***31***, 101551.
19. Hales, A., Prosser, R., Bravo Diaz, L., et al. (2020). The cell cooling coefficient as a design tool to optimise thermal management of lithium-ion cells in battery packs. eTransportation ***6***, 100089.
20. Shiao, H.C., Chua, D., Lin, H.-p., et al. (2000). Low temperature electrolytes for Li-ion PVDF cells. J. Power Sources ***87***, 167–173.
21. Li, W., Chen, S., Peng, X., et al. (2019). A comprehensive approach for the clustering of similar-performance cells for the design of a lithium-ion battery module for electric vehicles. Engineering ***38***, 795–803.
22. Qin, P., Sun, J., Yang, X., et al. (2021). Battery thermal management system based on the forced-air convection: a review. eTransportation ***7***, 100097.
23. Jaguemont, J., Boulon, L., and Dubé, Y. (2016). A comprehensive review of lithium-ion batteries used in hybrid and electric vehicles at cold temperatures. Appl. Energy ***164***, 99–114.
24. Wu, W., Wang, S., Wu, W., et al. (2019). A critical review of battery thermal performance and liquid based battery thermal management. Energy Convers. Manag. ***182***, 262–281.
25. Abdel-Monem, M., Trad, K., Omar, N., et al. (2017). Influence analysis of static and dynamic fast-charging current profiles on ageing performance of commercial lithium-ion batteries. Energy ***120***, 179–191.
26. Peng, X., Chen, S., Garg, A., et al. (2019). A review of the estimation and heating methods for lithium-ion batteries pack at the cold environment. Energy Sci. Eng. ***7***, 645–662.
27. Li, L., Xu, C., Chang, R., et al. (2021). Thermal-responsive, super-strong, ultrathin firewalls for quenching thermal runaway in high-energy battery modules. Energy Storage Mater. ***40***, 329–336.
28. Kim, J., Oh, J., and Lee, H. (2019). Review on battery thermal management system for electric vehicles. Appl. Therm. Eng. ***149***, 192–212.
29. Iten, M., Liu, S., and Shukla, A. (2016). A review on the air-PCM-TES application for free cooling and heating in the buildings. Renew. Sustain. Energy Rev. ***61***, 175–186.
30. Xia, G., Cao, L., and Bi, G. (2017). A review on battery thermal management in electric vehicle application. J. Power Sources ***367***, 90–105.
31. Burow, D., Sergeeva, K., Calles, S., et al. (2016). Inhomogeneous degradation of graphite anodes in automotive lithium ion batteries under low-temperature pulse cycling conditions. J. Power Sources ***307***, 806–814.
32. Nagasubramanian, G. (2001). Electrical characteristics of 18650 Li-ion cells at low temperatures. J. Appl. Electrochem. ***31***, 99–104.
33. Chen, S., Zhang, G., Wu, C., et al. (2022). Multi-objective optimization design for a double-direction liquid heating system-based Cell-to-Chassis battery module. Int. J. Heat Mass Tran. ***183***, 122184.
34. Zhang, G., Wei, X., Han, G., et al. (2021). Lithium plating on the anode for lithium-ion batteries during long-term low temperature cycling. J. Power Sources ***484***, 229312.
35. Väyrynen, A., and Salminen, J. (2012). Lithium ion battery production. J. Chem. Therm. ***46***, 80–85.
36. Zhang, S.S., Xu, K., and Jow, T.R. (2003). The low temperature performance of Li-ion batteries. J. Power Sources ***115***, 137–140.
37. You, H., Jiang, B., Zhu, J., et al. (2023). In-situ quantitative detection of irreversible lithium plating within full-lifespan of lithium-ion batteries. J. Power Sources ***564***, 232892.
38. Ng, B., Coman, P.T., Faegh, E., et al. (2020). Low-temperature lithium plating/corrosion hazard in lithium-ion batteries: electrode rippling, variable states of charge, and thermal and nonthermal runaway. ACS Appl. Energy Mater. ***3***, 3653–3664.
39. Wang, C.-Y., Zhang, G., Ge, S., et al. (2016). Lithium-ion battery structure that self-heats at low temperatures. Nature ***529***, 515–518.
40. Zhang, G.Y., Yang, M., Liu, B., et al. (2016). Rapid self-heating and internal temperature sensing of lithium-ion batteries at low temperatures. Electrochim. Acta ***313***, 149–161.
41. Park, G., Gunawardhana, N., Nakamura, H., et al. (2012). The study of electrochemical properties and lithium deposition of graphite at low temperature. J. Power Sources ***199***, 293–299.
42. Foss, C.E.L., Svensson, A.M., Gullbrekken, Ø., et al. (2018). Temperature effects on performance of graphite anodes in carbonate based electrolytes for lithium ion batteries. J. Energy Storage ***17***, 395–402.
43. Senyshyn, A., Mühlbauer, M., Dolotko, O., et al. (2015). Low-temperature performance of Li-ion batteries: the behavior of lithiated graphite. J. Power Sources ***282***, 235–240.
44. Zhu, J., Knapp, M., Liu, X., et al. (2021). Low-temperature separating lithium-ion battery interfacial polarization based on distribution of relaxation times (DRT) of impedance. Ann. Transl. Med. ***9***, 410–421.
45. Hu, X., Zheng, Y., Howey, D.A., et al. (2020). Battery warm-up methodologies at subzero temperatures for automotive applications: Recent advances and perspectives. Prog. Energy Combust. Sci. ***77***, 100806.
46. Smart, M.C., Ratnakumar, B.V., and Surampudi, S. (1999). Electrolytes for low-temperature lithium batteries based on ternary mixtures of aliphatic carbonates. J. Electrochem. Soc. ***146***, 486–492.
47. Ratnakumar, B.V., Smart, M.C., and Surampudi, S. (2001). Effects of SEI on the kinetics of lithium intercalation. J. Power Sources ***97–98***, 137–139.
48. Lin, H.P., Chua, D., Salomon, M., et al. (2001). Low-temperature behavior of Li-ion cells. Electrochem. Solid State Lett. ***4***, A71–A73.
49. Blomgren, G.E. (1999). Electrolytes for advanced batteries. J. Power Sources ***81–82***, 112–118.
50. Joho, F., Rykart, B., Imhof, R., et al. (1999). Key factors for the cycling stability of graphite intercalation electrodes for lithium-ion batteries. J. Power Sources ***81–82***, 243–247.
51. Amatucci, G., Du Pasquier, A., Blyr, A., et al. (1999). The elevated temperature performance of the LiMn2O4/C system: failure and solutions. Electrochim. Acta ***45***, 255–271.
52. Abe, K., Yoshitake, H., Kitakura, T., et al. (2004). Additives-containing functional electrolytes for suppressing electrolyte decomposition in lithium-ion batteries. Electrochim. Acta ***49***, 4613–4622.
53. Zhu, J., Wang, Y., Huang, Y., et al. (2022). Data-driven capacity estimation of commercial lithium-ion batteries from voltage relaxation. Nat. Commun. ***13***, 2261.
54. Vetter, J., Novák, P., Wagner, M.R., et al. (2005). Ageing mechanisms in lithium-ion batteries. J. Power Sources ***147***, 269–281.
55. Waldmann, T., Wilka, M., Kasper, M., et al. (2014). Temperature dependent ageing mechanisms in Lithium-ion batteries – A Post-Mortem study. J. Power Sources ***262***, 129–135.
56. Zhang, S.S., Xu, K., and Jow, T.R. (2002). Low temperature performance of graphite electrode in Li-ion cells. Electrochim. Acta ***48***, 241–246.
57. Gao, F., and Tang, Z. (2008). Kinetic behavior of LiFePO4/C cathode material for lithium-ion batteries. Electrochim. Acta ***53***, 5071–5075.
58. Yang, X.-G., Liu, T., and Wang, C.-Y. (2017). Innovative heating of large-size automotive Li-ion cells. J. Power Sources ***342***, 598–604.
59. Dai, H., Jiang, B., Hu, X., et al. (2021). Advanced battery management strategies for a sustainable energy future: Multilayer design concepts and research trends. Renew. Sustain. Energy Rev. ***138***, 110480.
60. Aricò, A.S., Bruce, P., Scrosati, B., et al. (2005). Nanostructured materials for advanced energy conversion and storage devices. Nat. Mater. ***4***, 366–377.
61. Sides, C.R., and Martin, C.R. (2005). Nanostructured electrodes and the low-temperature performance of Li-ion batteries. Adv. Mater. ***17***, 125–128.
62. Bruce, P.G., Scrosati, B., and Tarascon, J.-M. (2008). Nanomaterials for rechargeable lithium batteries. Angew. Chem. Int. Ed. Engl. ***47***, 2930–2946.
63. Wang, Y., and Cao, G. (2008). Developments in nanostructured cathode materials for high-performance lithium-ion batteries. Adv. Mater. ***20***, 2251–2269.
64. Wu, X.-L., Guo, Y.-G., Su, J., et al. (2013). Carbon-nanotube-decorated nano-LiFePO4 @C cathode material with superior high-rate and low-temperature performances for lithium-ion batteries. Adv. Energy Mater. ***3***, 1155–1160.
65. Kim, W., Ryu, W., Han, D., et al. (2014). Fabrication of graphene embedded LiFePO4 using a catalyst assisted self assembly method as a cathode material for high power lithium-ion batteries. ACS Appl. Mater. Interfaces ***6***, 4731–4736.
66. Yoon, S.-J., Myung, S.-T., and Sun, Y.-K. (2014). Low temperature electrochemical properties of Li[NixCoyMn1-x-y]O-2 cathode materials for lithium-ion batteries. J. Electrochem. Soc. ***161***, A1514–A1520.
67. Wu, Y., Jiang, C., Wan, C., et al. (2002). Modified natural graphite as anode material for lithium ion batteries. J. Power Sources ***111***, 329–334.
68. Nobili, F., Mancini, M., Dsoke, S., et al. (2010). Low-temperature behavior of graphite–tin composite anodes for Li-ion batteries. J. Power Sources ***195***, 7090–7097.
69. Gao, J., Fu, L.J., Zhang, H.P., et al. (2006). Suppression of PC decomposition at the surface of graphitic carbon by Cu coating. Electrochem. Commun. ***8***, 1726–1730.
70. Raccichini, R., Varzi, A., Chakravadhanula, V.S.K., et al. (2015). Enhanced low-temperature lithium storage performance of multilayer graphene made through an improved ionic liquid-assisted synthesis. J. Power Sources ***281***, 318–325.
71. Edström, K., Gustafsson, T., and Thomas, J.O. (2004). The cathode–electrolyte interface in the Li-ion battery. Electrochim. Acta ***50***, 397–403.
72. Aurbach, D., Zinigrad, E., Cohen, Y., et al. (2002). A short review of failure mechanisms of lithium metal and lithiated graphite anodes in liquid electrolyte solutions. Solid State Ionics ***148***, 405–416.
73. Churikov, A.V. (2001). Transfer mechanism in solid-electrolyte layers on lithium: influence of temperature and polarization. Electrochim. Acta ***46***, 2415–2426.
74. Zhong, Z., Chen, L., Zhu, C., et al. (2020). Nano LiFePO4 coated Ni rich composite as cathode for lithium ion batteries with high thermal ability and excellent cycling performance. J. Power Sources ***464***, 228235.
75. Marinaro, M., Pfanzelt, M., Kubiak, P., et al. (2011). Low temperature behaviour of TiO2 rutile as negative electrode material for lithium-ion batteries. J. Power Sources ***196***, 9825–9829.
76. Negi, R.S., Celik, E., Pan, R., et al. (2021). Insights into the positive effect of post-annealing on the electrochemical performance of Al2O3-coated Ni-Rich NCM cathodes for lithium-ion batteries. ACS Appl. Energy Mater. ***4***, 3369–3380.
77. Andersson, A.M., Henningson, A., Siegbahn, H., et al. (2003). Electrochemically lithiated graphite characterised by photoelectron spectroscopy. J. Power Sources ***119–121***, 522–527.
78. Ji, H., Zhang, L., Pettes, M.T., et al. (2012). Ultrathin graphite foam: a three-dimensional conductive network for battery electrodes. Nano Lett. ***12***, 2446–2451.

79. Wang, L., Wang, H., Liu, Z., et al. (2010). A facile method of preparing mixed conducting LiFePO4/graphene composites for lithium-ion batteries. Solid State Ionics ***181***, 1685–1689.
80. Ravet, N., Chouinard, Y., Magnan, J.F., et al. (2001). Electroactivity of natural and synthetic triphylite. J. Power Sources ***97–98***, 503–507.
81. Ji, H.-X., Wu, X.-L., Fan, L.-Z., et al. (2010). Self-wound composite nanomembranes as electrode materials for lithium ion batteries. Adv. Mater. ***22***, 4591–4595.
82. Chang, Z.-R., Lv, H.-J., Tang, H.-W., et al. (2009). Synthesis and characterization of high-density LiFePO4/C composites as cathode materials for lithium-ion batteries. Electrochim. Acta ***54***, 4595–4599.
83. Hu, Y., Doeff, M.M., Kostecki, R., et al. (2004). Electrochemical performance of sol-gel synthesized LiFePO4 in lithium batteries. J. Electrochem. Soc. ***151***, A1279–A1285.
84. Doeff, M., Wilcox, J., Kostecki, R., et al. (2006). Optimization of carbon coatings on LiFePO4. Meet. Abstr. ***163***, 180–184.
85. Park, O.K., Cho, Y., Lee, S., et al. (2011). Who will drive electric vehicles, olivine or spinel? Energy Environ. Sci. ***4***, 1621–1633.
86. Nien, Y.-H., Carey, J.R., and Chen, J.-S. (2009). Physical and electrochemical properties of LiFePO4/C composite cathode prepared from various polymer-containing precursors. J. Power Sources ***193***, 822–827.
87. Wu, X.-L., Jiang, L.-Y., Cao, F.-F., et al. (2009). LiFePO4 nanoparticles embedded in a nanoporous carbon matrix: superior cathode material for electrochemical energy-storage devices. Adv. Mater. ***21***, 2710–2714.
88. Ellis, B., Subramanya Herle, P., Rho, Y.H., et al. (2007). Nanostructured materials for lithium-ion batteries: Surface conductivity vs. bulk ion/electron transport. Faraday Discuss ***134***, 119–141. discussion 215-233, 415-419.
89. Yuan, L.X., Wang, Z.H., Zhang, W.X., et al. (2011). Development and challenges of LiFePO4 cathode material for lithium-ion batteries. Energy Environ. Sci. ***4***, 269–284.
90. Li, W.-H., Li, Y.-M., Liu, X.-F., et al. (2022). All-climate and ultrastable dual-ion batteries with long life achieved via synergistic enhancement of cathode and anode interfaces. Adv. Funct. Mater. ***32***, 2201038.
91. Chang, Y.-C., Peng, C.-T., and Hung, I.M. (2014). Effects of particle size and carbon coating on electrochemical properties of LiFePO4/C prepared by hydrothermal method. J. Mater. Sci. ***49***, 6907–6916.
92. Song, X., Liu, G., Yue, H., et al. (2021). A novel low-cobalt long-life LiNi0.88Co0.06Mn0.03Al0.03O2 cathode material for lithium ion batteries. Chem. Eng. J. ***407***, 126301.
93. Smart, M.C., Whitacre, J.F., Ratnakumar, B.V., et al. (2007). Electrochemical performance and kinetics of Li1+x(Co1/3Ni1/3Mn1/3)1−xO2 cathodes and graphite anodes in low-temperature electrolytes. J. Power Sources ***168***, 501–508.
94. Rui, X.H., Jin, Y., Feng, X.Y., et al. (2011). A comparative study on the low-temperature performance of LiFePO4/C and Li3V2(PO4)3/C cathodes for lithium-ion batteries. J. Power Sources ***196***, 2109–2114.
95. Petibon, R., Harlow, J., Le, D.B., et al. (2015). The use of ethyl acetate and methyl propanoate in combination with vinylene carbonate as ethylene carbonate-free solvent blends for electrolytes in Li-ion batteries. Electrochim. Acta ***154***, 227–234.
96. Smart, M.C., Ratnakumar, B.V., Chin, K.B., et al. (2010). Lithium-ion electrolytes containing ester cosolvents for improved low temperature performance. J. Electrochem. Soc. ***157***, A1361.
97. Zhou, L., Xu, M., and Lucht, B.L. (2013). Performance of lithium tetrafluorooxalatophosphate in methyl butyrate electrolytes. J. Appl. Electrochem. ***43***, 497–505.
98. Deng, X., Zhang, S., Chen, C., et al. (2022). Rational design of electrolytes operating at low temperatures: does the co-solvent with a lower melting point correspond to better performance? Electrochim. Acta ***415***, 140268.
99. Smart, M.C., Lucht, B.L., Dalavi, S., et al. (2012). The effect of additives upon the performance of MCMB/LiNixCo1−xO2Li-ion cells containing methyl butyrate-based wide operating temperature range electrolytes. J. Electrochem. Soc. ***159***, A739–A751.
100. Niedzicki, L., Grugeon, S., Laruelle, S., et al. (2011). New covalent salts of the 4+V class for Li batteries. J. Power Sources ***196***, 8696–8700.
101. Xu, K., Zhang, S., and Jow, T.R. (2005). LiBOB as additive in LiPF[sub 6]-based lithium ion electrolytes. Electrochem. Solid State Lett. ***8***, A365.
102. Lazar, M.L., and Lucht, B.L. (2015). Carbonate free electrolyte for lithium ion batteries containing γ-butyrolactone and methyl butyrate. J. Electrochem. Soc. ***162***, A928–A934.
103. Li, S., Zhao, W., Zhou, Z., et al. (2014). Studies on electrochemical performances of novel electrolytes for wide-temperature-range lithium-ion batteries. ACS Appl. Mater. Interfaces ***6***, 4920–4926.
104. Zhang, N., Deng, T., Zhang, S., et al. (2022). Critical review on low-temperature Li-ion/metal batteries. Adv. Mater. ***34***, 2107899.
105. Herreyre, S., Huchet, O., Barusseau, S., et al. (2001). New Li-ion electrolytes for low temperature applications. J. Power Sources ***97–98***, 576–580.
106. Plichta, E.J., and Behl, W.K. (2000). A low-temperature electrolyte for lithium and lithium-ion batteries. J. Power Sources ***88***, 192–196.
107. Ji, Y., Zhang, Y., and Wang, C.-Y. (2013). Li-ion cell operation at low temperatures. J. Electrochem. Soc. ***160***, A636–A649.
108. Yang, B., Zhang, H., Yu, L., et al. (2016). Lithium difluorophosphate as an additive to improve the low temperature performance of LiNi0.5Co0.2Mn0.3O2/graphite cells. Electrochimica Acta ***221***, 107–114.
109. Liu, Y.-K., Zhao, C.-Z., Du, J., et al. (2023). Research progresses of liquid electrolytes in lithium-ion batteries. Small ***19***, 2205315.
110. Goodenough, J.B., and Kim, Y. (2010). Challenges for rechargeable Li batteries. Chem. Mater. ***22***, 587–603.
111. Li, Q., Lu, D., Zheng, J., et al. (2017). Li+-desolvation dictating lithium-ion battery's low-temperature performances. ACS Appl. Mater. Interfaces ***9***, 42761–42768.
112. Li, Q., Jiao, S., Luo, L., et al. (2017). Wide-temperature electrolytes for lithium-ion batteries. ACS Appl. Mater. Interfaces ***9***, 18826–18835.
113. Zhang, S.S., Xu, K., and Jow, T.R. (2006). EIS study on the formation of solid electrolyte interface in Li-ion battery. Electrochim. Acta ***51***, 1636–1640.
114. Liao, X.-Z., Ma, Z.-F., Gong, Q., et al. (2008). Low-temperature performance of LiFePO4/C cathode in a quaternary carbonate-based electrolyte. Electrochem. Commun. ***10***, 691–694.
115. Mandal, B.K., Padhi, A.K., Shi, Z., et al. (2006). New low temperature electrolytes with thermal runaway inhibition for lithium-ion rechargeable batteries. J. Power Sources ***162***, 690–695.
116. Lin, S., Hua, H., Lai, P., et al. (2021). A multifunctional dual-salt localized high-concentration electrolyte for fast dynamic high-voltage lithium battery in wide temperature range. Adv. Energy Mater. ***11***, 2101775.
117. Zhang, S.S., Xu, K., and Jow, T.R. (2002). A new approach toward improved low temperature performance of Li-ion battery. Electrochem. Commun. ***4***, 928–932.
118. Jow, T.R., Ding, M.S., Xu, K., et al. (2003). Nonaqueous electrolytes for wide-temperature-range operation of Li-ion cells. J. Power Sources ***119–121***, 343–348.
119. Abraham, D.P., Heaton, J.R., Kang, S.H., et al. (2008). Investigating the low-temperature impedance increase of lithium-ion cells. J. Electrochem. Soc. ***155***, A41.
120. Huang, C.K., Sakamoto, J.S., Wolfenstine, J., et al. (2000). Limits of low-temperature performance of Li-ion cells. J. Electrochem. Soc. ***147***, 2893–2896.
121. Du, Y.-F., Sun, G.-H., Li, Y., et al. (2021). Pre-oxidation of lignin precursors for hard carbon anode with boosted lithium-ion storage capacity. Carbon ***178***, 243–255.
122. Nobili, F., Dsoke, S., Mecozzi, T., et al. (2005). Metal-oxidized graphite composite electrodes for lithium-ion batteries. Electrochim. Acta ***51***, 536–544.
123. Mancini, M., Nobili, F., Dsoke, S., et al. (2009). Lithium intercalation and interfacial kinetics of composite anodes formed by oxidized graphite and copper. J. Power Sources ***190***, 141–148.
124. Cao, X., Kim, J.H., and Oh, S.M. (2002). The effects of oxidation on the surface properties of MCMB-6-28. Electrochim. Acta ***47***, 4085–4089.
125. Collins, G.A., Geaney, H., and Ryan, K.M. (2021). Alternative anodes for low temperature lithium-ion batteries. J. Mater. Chem. A Mater. ***9***, 14172–14213.
126. Shi, H.W., Yang, J.G., Wang, Y., et al. (2020). In situ fabrication of dual coating structured SiO/1D-C/a-C composite as high-performance lithium ion battery anode by fluidized bed chemical vapor deposition. Carbon ***168***, 113–124.
127. Wang, G.J., Gao, J., Fu, L.J., et al. (2007). Preparation and characteristic of carbon-coated Li4Ti5O12 anode material. J. Power Sources ***174***, 1109–1112.
128. Zou, M., Li, J., Wen, W., et al. (2014). Silver-incorporated composites of Fe2O3 carbon nanofibers as anodes for high-performance lithium batteries. J. Power Sources ***270***, 468–474.
129. Li, J., Wen, W., Xu, G., et al. (2015). Fe-added Fe3C carbon nanofibers as anode for Li ion batteries with excellent low-temperature performance. Electrochim. Acta ***153***, 300–305.
130. Yang, M., Sun, Z., Nie, P., et al. (2022). SbPS4: A novel anode for high-performance sodium-ion batteries. Chin. Chem. Lett. ***33***, 470–474.
131. Yuan, T., Cai, R., Wang, K., et al. (2009). Combustion synthesis of high-performance Li4Ti5O12 for secondary Li-ion battery. Ceram. Int. ***35***, 1757–1768.
132. Wen, Z., Yang, X., and Huang, S. (2007). Composite anode materials for Li-ion batteries. J. Power Sources ***174***, 1041–1045.
133. Aurbach, D. (2000). Review of selected electrode–solution interactions which determine the performance of Li and Li ion batteries. J. Power Sources ***89***, 206–218.
134. Piao, N., Gao, X., Yang, H., et al. (2022). Challenges and development of lithium-ion batteries for low temperature environments. eTransportation ***11***, 100145.
135. Lei, Z., Zhang, Y., and Lei, X. (2018). Improving temperature uniformity of a lithium-ion battery by intermittent heating method in cold climate. Int. J. Heat Mass Tran. ***121***, 275–281.
136. Chen, S., Peng, X., Bao, N., et al. (2019). A comprehensive analysis and optimization process for an integrated liquid cooling plate for a prismatic lithium-ion battery module. Appl. Therm. Eng. ***156***, 324–339.
137. Li, S., Kirkaldy, N., Zhang, C., et al. (2021). Optimal cell tab design and cooling strategy for cylindrical lithium-ion batteries. J. Power Sources ***492***, 229594.
138. Lin, J., Liu, X., Li, S., et al. (2021). A review on recent progress, challenges and perspective of battery thermal management system. Int. J. Heat Mass Tran. ***167***, 120834.
139. Song, H.S., Jeong, J.B., Lee, B.H., et al. (2012). Experimental study on the effects of preheating a battery in a low-temperature environment. In 2012 IEEE Vehicle Power and Propulsion Conference (VPPC).
140. Zhang, X., Kong, X., Li, G., et al. (2014). Thermodynamic assessment of active cooling/heating methods for lithium-ion batteries of electric vehicles in extreme conditions. Energy ***64***, 1092–1101.
141. Zhang, X., Li, Z., Luo, L., et al. (2022). A review on thermal management of lithium-ion batteries for electric vehicles. Energy ***238***, 121652.
142. Nelson, P., Dees, D., Amine, K., et al. (2002). Modeling thermal management of lithium-ion PNGV batteries. J. Power Sources ***110***, 349–356.
143. Wang, Q., Jiang, B., Xue, Q.F., et al. (2015). Experimental investigation on EV battery cooling and heating by heat pipes. Appl. Therm. Eng. ***88***, 54–60.
144. Luo, M., Song, J., Ling, Z., et al. (2021). Phase change material coat for battery thermal management with integrated rapid heating and cooling functions from −40 °C to 50 °C. Mater. Today Energy ***20***, 100652.

145. Zhong, G., Zhang, G., Yang, X., et al. (2017). Researches of composite phase change material cooling/resistance wire preheating coupling system of a designed 18650-type battery module. Appl. Therm. Eng. ***127***, 176–183.
146. Ling, Z., Wen, X., Zhang, Z., et al. (2018). Thermal management performance of phase change materials with different thermal conductivities for Li-ion battery packs operated at low temperatures. Energy ***144***, 977–983.
147. Pan, S., Zheng, Y., Lu, L., et al. (2023). Neural network PID-based preheating control and optimization for a li-ion battery module at low temperatures. World Electric Vehicle J. ***14***, 83.
148. Lin, C.T., Lai, K.L., Tian, Y., et al. (2022). Heating lithium-ion batteries at low temperatures for onboard applications: recent progress, challenges and prospects. J. Med. Ultrasound ***30***, 3–5.
149. Li, J., and Huang, W. (2014). Background: correlating microscale and macroscale. In Towards Mesoscience: The Principle of Compromise in Competition, J. Li and W. Huang, eds. (Springer Berlin Heidelberg), pp. 1–6.
150. Fan, R., Zhang, C., Wang, Y., et al. (2019). Numerical study on the effects of battery heating in cold climate. J. Energy Storage ***26***, 100969.
151. Huang, R., Wang, X., Jiang, B., et al. (2023). Revealing the electrochemical impedance characteristics of lithium-ion battery (nickel-cobalt-aluminum vs. graphite) under various alternating current amplitudes. J. Power Sources ***566***, 232929.
152. Yue, Q.L., He, C.X., Wu, M.C., et al. (2021). Advances in thermal management systems for next-generation power batteries. Int. J. Heat Mass Tran. ***181***, 121853.
153. Qu, Z.G., Jiang, Z.Y., and Wang, Q. (2019). Experimental study on pulse self–heating of lithium–ion battery at low temperature. Int. J. Heat Mass Tran. ***135***, 696–705.
154. Zhang, J., Ge, H., Li, Z., et al. (2015). Internal heating of lithium-ion batteries using alternating current based on the heat generation model in frequency domain. J. Power Sources ***273***, 1030–1037.
155. Zhao, X.W., Zhang, G.Y., Yang, L., et al. (2011). A new charging mode of Li-ion batteries with LiFePO4/C composites under low temperature. J. Therm. Anal. Calorim. ***104***, 561–567.
156. Ruan, H., Jiang, J., Sun, B., et al. (2016). A rapid low-temperature internal heating strategy with optimal frequency based on constant polarization voltage for lithium-ion batteries. Appl. Energy ***177***, 771–782.
157. Ji, Y., and Wang, C.Y. (2013). Heating strategies for Li-ion batteries operated from subzero temperatures. Electrochim. Acta ***107***, 664–674.
158. Wu, H., Zhang, X., Cao, R., et al. (2021). An investigation on electrical and thermal characteristics of cylindrical lithium-ion batteries at low temperatures. Energy ***225***, 120223.
159. Brodd, R.J. (2012). Batteries for Sustainability: Selected Entries from the Encyclopedia of Sustainability Science and Technology (Springer Science & Business Media).
160. Chen, S., Bao, N., Garg, A., et al. (2021). A fast charging–cooling coupled scheduling method for a liquid cooling-based thermal management system for lithium-ion batteries. Engineering ***7***, 1165–1176.
161. Chen, S., Bao, N., Gao, L., et al. (2020). An experimental investigation of liquid cooling scheduling for a battery module. Int. J. Energy Res. ***44***, 3020–3032.
162. Chen, S., Wei, X., Garg, A., et al. (2021). A comprehensive flowrate optimization design for a novel air-liquid cooling coupled battery thermal management system. J. Electrochem. Energy Convers. Storage ***18***, 021008.
163. Shen, K., Sun, J., Zheng, Y., et al. (2022). A comprehensive analysis and experimental investigation for the thermal management of cell-to-pack battery system. Appl. Therm. Eng. ***211***, 118422.
164. Chen, S., Garg, A., Gao, L., et al. (2021). An experimental investigation for a hybrid phase change material-liquid cooling strategy to achieve high-temperature uniformity of Li-ion battery module under fast charging. Int. J. Energy Res. ***45***, 6198–6212.
165. Wang, Y., Feng, X., Peng, Y., et al. (2022). Reductive gas manipulation at early self-heating stage enables controllable battery thermal failure. Joule ***6***, 2810–2820.
166. Kong, D., Wang, G., Ping, P., et al. (2022). A coupled conjugate heat transfer and CFD model for the thermal runaway evolution and jet fire of 18650 lithium-ion battery under thermal abuse. eTransportation ***12***, 100157.
167. Wang, G., Kong, D., Ping, P., et al. (2023). Revealing particle venting of lithium-ion batteries during thermal runaway: a multi-scale model toward multiphase process. eTransportation ***16***, 100237.
168. Ping, P., Wang, Q., Huang, P., et al. (2015). Study of the fire behavior of high-energy lithium-ion batteries with full-scale burning test. J. Power Sources ***285***, 80–89.
169. Li, K., Xu, C., Wang, H., et al. (2022). Investigation for the effect of side plates on thermal runaway propagation characteristics in battery modules. Appl. Therm. Eng. ***201***, 117774.
170. Chen, M., He, Y., De Zhou, C., et al. (2016). Experimental study on the combustion characteristics of primary lithium batteries fire. Fire Technol. ***52***, 365–385.
171. Wang, Y., Song, Z., Wang, H., et al. (2023). Experimental research on flammability characteristics and ignition conditions of hybrid mixture emissions venting from a large format thermal failure lithium-ion battery. J. Energy Storage ***59***, 106466.
172. Ouyang, D., Liu, J., Chen, M., et al. (2018). An experimental study on the thermal failure propagation in lithium-ion battery pack. J. Electrochem. Soc. ***165***, A2184–A2193.
173. Lamb, J., Orendorff, C.J., Steele, L.A.M., et al. (2015). Failure propagation in multi-cell lithium ion batteries. J. Power Sources ***283***, 517–523.
174. Hu, J., Liu, T., Wang, X., et al. (2022). Investigation on thermal runaway of 18,650 lithium ion battery under thermal abuse coupled with charging. J. Energy Storage ***51***, 104482.
175. Liu, T., Hu, J., Zhu, X., et al. (2022). A practical method of developing cooling control strategy for thermal runaway propagation prevention in lithium ion battery modules. J. Energy Storage ***50***, 104564.
176. Xu, C., Wang, H., Jiang, F., et al. (2023). Modelling of thermal runaway propagation in lithium-ion battery pack using reduced-order model. Energy ***268***, 126646.
177. Feng, X., Lu, L., Ouyang, M., et al. (2016). A 3D thermal runaway propagation model for a large format lithium ion battery module. Energy ***115***, 194–208.
178. Feng, X., Sun, J., Ouyang, M., et al. (2015). Characterization of penetration induced thermal runaway propagation process within a large format lithium ion battery module. J. Power Sources ***275***, 261–273.
179. Wang, Q., Mao, B., Stoliarov, S.I., et al. (2019). A review of lithium ion battery failure mechanisms and fire prevention strategies. Prog. Energy Combust. Sci. ***73***, 95–131.
180. Huang, P., Ping, P., Li, K., et al. (2016). Experimental and modeling analysis of thermal runaway propagation over the large format energy storage battery module with Li4Ti5O12 anode. Appl. Energy ***183***, 659–673.
181. Zhang, W., Wu, J., Li, Y., et al. (2022). High stability and high performance nitrogen doped carbon containers for lithium-ion batteries. J. Colloid Interface Sci. ***625***, 692–699.
182. MacNeil, D.D., Larcher, D., and Dahn, J.R. (1999). Comparison of the reactivity of various carbon electrode materials with electrolyte at elevated temperature. J. Electrochem. Soc. ***146***, 3596–3602.
183. Richard, M.N., and Dahn, J.R. (1999). Accelerating rate calorimetry study on the thermal stability of lithium intercalated graphite in electrolyte. I. experimental. J. Electrochem. Soc. ***146***, 2068–2077.
184. Yang, H., Amiruddin, S., Bang, H.J., et al. (2006). A review of Li-ion cell chemistries and their potential use in hybrid electric vehicles. J. Ind. Eng. Chem. ***12***, 12–38.
185. Abraham, D.P., Roth, E.P., Kostecki, R., et al. (2006). Diagnostic examination of thermally abused high-power lithium-ion cells. J. Power Sources ***161***, 648–657.
186. Wang, Q., Sun, J., Yao, X., et al. (2006). Thermal behavior of lithiated graphite with electrolyte in lithium-ion batteries. J. Electrochem. Soc. ***153***, A329–A333.
187. Wang, Q., Sun, J., Yao, X., et al. (2006). Micro calorimeter study on the thermal stability of lithium-ion battery electrolytes. J. Loss Prev. Process. Ind. ***19***, 561–569.
188. Al Hallaj, S., Maleki, H., Hong, J.S., et al. (1999). Thermal modeling and design considerations of lithium-ion batteries. J. Power Sources ***83***, 1–8.
189. Arora, S., Shen, W., and Kapoor, A. (2016). Review of mechanical design and strategic placement technique of a robust battery pack for electric vehicles. Renew. Sustain. Energy Rev. ***60***, 1319–1331.
190. Mao, B., Chen, H., Cui, Z., et al. (2018). Failure mechanism of the lithium ion battery during nail penetration. Int. J. Heat Mass Tran. ***122***, 1103–1115.
191. Zhang, G., Wei, X., Chen, S., et al. (2021). Comprehensive investigation of a slight overcharge on degradation and thermal runaway behavior of lithium-ion batteries. ACS Appl. Mater. Interfaces ***13***, 35054–35068.
192. Feng, X., He, X., Ouyang, M., et al. (2015). Thermal runaway propagation model for designing a safer battery pack with 25Ah LiNixCoyMnzO2 large format lithium ion battery. Appl. Energy ***154***, 74–91.
193. Liu, X., Ren, D., Hsu, H., et al. (2018). Thermal runaway of lithium-ion batteries without internal short circuit. Joule ***2***, 2047–2064.
194. Lisbona, D., and Snee, T. (2011). A review of hazards associated with primary lithium and lithium-ion batteries. Process Saf. Environ. Protect. ***89***, 434–442.
195. Wu, C., Wu, Y., Feng, X., et al. (2022). Ultra-high temperature reaction mechanism of LiNi0.8Co0.1Mn0.1O2 electrode. J. Energy Storage ***52***, 104870.
196. Wang, Y., Ren, D., Feng, X., et al. (2022). Thermal runaway modeling of large format high-nickel/silicon-graphite lithium-ion batteries based on reaction sequence and kinetics. Appl. Energy ***306***, 117943.
197. Yang, H., and Shen, X.-D. (2007). Dynamic TGA–FTIR studies on the thermal stability of lithium/graphite with electrolyte in lithium-ion cell. J. Power Sources ***167***, 515–519.
198. Kawamura, T., Kimura, A., Egashira, M., et al. (2002). Thermal stability of alkyl carbonate mixed-solvent electrolytes for lithium ion cells. J. Power Sources ***104***, 260–264.
199. Wang, Q., Sun, J., Yao, X., et al. (2005). Thermal stability of LiPF6/EC+DEC electrolyte with charged electrodes for lithium ion batteries. Thermochim. Acta ***437***, 12–16.
200. Gnanaraj, J.S., Zinigrad, E., Asraf, L., et al. (2003). The use of accelerating rate calorimetry (ARC) for the study of the thermal reactions of Li-ion battery electrolyte solutions. J. Power Sources ***119–121***, 794–798.
201. Xu, C., Zhang, F., Feng, X., et al. (2021). Experimental study on thermal runaway propagation of lithium-ion battery modules with different parallel-series hybrid connections. J. Clean. Prod. ***284***, 124749.
202. Zhang, G., Wei, X., Chen, S., et al. (2021). Revealing the impact of slight electrical abuse on the thermal safety characteristics for lithium-ion batteries. ACS Appl. Energy Mater. ***4***, 12858–12870.
203. Wang, Y., Ren, D., Feng, X., et al. (2021). Thermal kinetics comparison of delithiated Li[NixCoyMn1-x-y]O2 cathodes. J. Power Sources ***514***, 230582.
204. Balakrishnan, P.G., Ramesh, R., and Prem Kumar, T. (2006). Safety mechanisms in lithium-ion batteries. J. Power Sources ***155***, 401–414.
205. Feng, X., Ren, D., He, X., et al. (2020). Mitigating thermal runaway of lithium-ion batteries. Joule ***4***, 743–770.
206. Rui, X., Feng, X., Wang, H., et al. (2021). Synergistic effect of insulation and liquid cooling on mitigating the thermal runaway propagation in lithium-ion battery module. Appl. Therm. Eng. ***199***, 117521.
207. Xu, G.-L., Liu, Q., Lau, K.K.S., et al. (2019). Building ultraconformal protective layers on both secondary and primary particles of layered lithium transition metal oxide cathodes. Nat. Energy ***4***, 484–494.
208. Hou, P., Zhang, H., Deng, X., et al. (2017). Stabilizing the electrode/electrolyte interface of LiNi0.8Co0.15Al0.05O2 through tailoring aluminum distribution in microspheres as long-

life, high-rate, and safe cathode for lithium-ion batteries. ACS Appl. Mater. Interfaces **9**, 29643–29653.
209. Zhang, G., Wei, X., Tang, X., et al. (2021). Internal short circuit mechanisms, experimental approaches and detection methods of lithium-ion batteries for electric vehicles: A review. Renew. Sustain. Energy Rev. **141**, 110790.
210. Rahman, M.M., Mateti, S., Cai, Q., et al. (2019). High temperature and high rate lithium-ion batteries with boron nitride nanotubes coated polypropylene separators. Energy Storage Mater. **19**, 352–359.
211. Wu, X., Wang, Z., He, Z., et al. (2021). Development of cathode-electrolyte-interphase for safer lithium batteries. Energy Storage Mater. **37**, 77–86.
212. Friesen, A., Hildebrand, S., Horsthemke, F., et al. (2017). Al2O3 coating on anode surface in lithium ion batteries: impact on low temperature cycling and safety behavior. J. Power Sources **363**, 70–77.
213. Hou, J., Wang, L., Feng, X., et al. (2023). Thermal runaway of lithium-ion batteries employing flame-retardant fluorinated electrolytes. Energy Environ. Mater. **6**, e12297.
214. Wu, C., Wu, Y., Yang, X., et al. (2021). Thermal runaway suppression of high-energy lithium-ion batteries by designing the stable interphase. J. Electrochem. Soc. **168**, 090563.
215. Ma, L., Xia, J., Xia, X., et al. (2014). The impact of vinylene carbonate, fluoroethylene carbonate and vinyl ethylene carbonate electrolyte additives on electrode/electrolyte reactivity studied using accelerating rate calorimetry. J. Electrochem. Soc. **161**, A1495–A1498.
216. Liu, K., Liu, Y., Lin, D., et al. (2018). Materials for lithium-ion battery safety. Sci. Adv. **4**, eaas9820.
217. Hou, J., Wang, L., Feng, X., et al. (2023). Thermal runaway of lithium-ion batteries employing flame-retardant fluorinated electrolytes. Energy Environm. Mater. **6**, e12297.
218. Wang, H., Du, Z., Rui, X., et al. (2020). A comparative analysis on thermal runaway behavior of Li (NixCoyMnz) O2 battery with different nickel contents at cell and module level. J. Hazard Mater. **393**, 122361.
219. Zhang, F., Feng, X., Xu, C., et al. (2022). Thermal runaway front in failure propagation of long-shape lithium-ion battery. Int. J. Heat Mass Tran. **182**, 121928.
220. Noelle, D.J., Shi, Y., Wang, M., et al. (2018). Aggressive electrolyte poisons and multifunctional fluids comprised of diols and diamines for emergency shutdown of lithium-ion batteries. J. Power Sources **384**, 93–97.
221. Ji, W., Jiang, B., Ai, F., et al. (2015). Temperature-responsive microspheres-coated separator for thermal shutdown protection of lithium ion batteries. RSC Adv. **5**, 172–176.
222. Shi, Y., Noelle, D.J., Wang, M., et al. (2017). Mitigating thermal runaway of lithium-ion battery through electrolyte displacement. Appl. Phys. Lett. **110**, 063902.
223. Naguib, M., Allu, S., Simunovic, S., et al. (2018). Limiting internal short-circuit damage by electrode partition for impact-tolerant Li-ion batteries. Joule **2**, 155–167.
224. Liu, K., Liu, W., Qiu, Y., et al. (2017). Electrospun core-shell microfiber separator with thermal-triggered flame-retardant properties for lithium-ion batteries. Sci. Adv. **3**, e1601978.
225. Lai, X., Meng, Z., Zhang, F., et al. (2023). Mitigating thermal runaway hazard of high-energy lithium-ion batteries by poison agent. J. Energy Chem. **83**, 3–15.
226. Hong, Y., Zhang, Y., Li, C., et al. (2023). High-security prismatic battery with cover filled agent. J. Energy Storage **64**, 107133.
227. Lu, L., Han, X., Li, J., et al. (2013). A review on the key issues for lithium-ion battery management in electric vehicles. J. Power Sources **226**, 272–288.
228. Jin, C., Sun, Y., Wang, H., et al. (2021). Model and experiments to investigate thermal runaway characterization of lithium-ion batteries induced by external heating method. J. Power Sources **504**, 230065.
229. Qian, L., Yi, Y., Zhang, W., et al. (2023). Revealing the impact of high current overcharge/overdischarge on the thermal safety of degraded Li-ion batteries. Int. J. Energy Res. **2023**, 8571535.
230. Wu, H., Chen, S., Chen, J., et al. (2022). Dimensionless normalized concentration based thermal-electric regression model for the thermal runaway of lithium-ion batteries. J. Power Sources **521**, 230958.
231. Huang, W., Feng, X., Pan, Y., et al. (2023). Early warning of battery failure based on venting signal. J. Energy Storage **59**, 106536.
232. Cai, T., Valecha, P., Tran, V., et al. (2021). Detection of Li-ion battery failure and venting with carbon dioxide sensors. eTransportation **7**, 100100.
233. Li, W., Wang, H., Zhang, Y., et al. (2019). Flammability characteristics of the battery vent gas: A case of NCA and LFP lithium-ion batteries during external heating abuse. J. Energy Storage **24**, 100775.
234. Yang, X., Wang, H., Li, M., et al. (2022). Experimental study on thermal runaway behavior of lithium-ion battery and analysis of combustible limit of gas production. Batteries **8**, 250.
235. Li, L., Jia, C., Liu, Y., et al. (2022). Nanograin-glass dual-phasic, elasto-flexible, fatigue-tolerant, and heat-insulating ceramic sponges at large scales. Mater. Today **54**, 72–82.
236. Shen, K., Sun, J., Xu, C., et al. (2023). Experimental investigation for the phase change material barrier area effect on the thermal runaway propagation prevention of cell-to-pack batteries. Batteries **9**, 206.

ACKNOWLEDGMENTS

This work is supported by National Natural Science Foundation of China (NSFC) (nos. U20A20310, 52176199, and 52076121), sponsored by Program of Shanghai Academic/Technology Research Leader(22XD1423800).

AUTHOR CONTRIBUTIONS

H.D. and X.F. supervised the manuscript. S.C. wrote and edited the manuscript. All authors contributed to the article and approved the submitted version.

DECLARATION OF INTERESTS

The authors declare no competing interests.

SUPPLEMENTAL INFORMATION

It can be found online at https://doi.org/10.1016/j.xinn.2023.100465.

LEAD CONTACT WEBSITE

https://auto.tongji.edu.cn/info/1146/6301.htm